**RIGA TECHNICAL UNIVERSITY**
Faculty of Electrical and Environmental Engineering
Institute of Power Engineering

**Ivars Zālītis**
Doctoral Student of the Study Programme "Power Engineering"

# APPLICATION OF ESTIMATION OF MODEL PARAMETERS FOR PROTECTIVE AUTOMATION OF TRANSMISSION LINES

**Summary of the Doctoral Thesis**

Scientific supervisor
Associate Professor Dr. sc. ing.
ALEKSANDRS DOLGICERS

RTU Press
Riga 2020

Zālītis, I. Application of Estimation of Model Parameters for Protective Automation of Transmission Lines. Summary of the Doctoral Thesis. Riga: RTU Press, 2020. 56 p.

Published in accordance with the decision of the Promotion Council "RTU P-05" of 16 July 2020, Minutes No. 75/20.

This research has been supported by the Latvian Council of Science, project: Management and Operation of an Intelligent Power System (I-POWER) (No. lzp-2018/1-0066) and by National Research Programme project: Innovative Intelligent Network Technologies and their Optimization (INGRIDO). 2018 – 2021.

This research was funded by the Ministry of Economics of the Republic of Latvia, project "Trends, Challenges and Solutions of Latvian Gas Infrastructure Development (LAGAS)", project No. VPP-EM-INFRA-2018/1-0003.



**ISBN 978-9934-22-495-9 (print)**
**ISBN 978-9934-22-496-6 (pdf)**

# DOCTORAL THESIS PROPOSED TO RIGA TECHNICAL UNIVERSITY FOR THE PROMOTION TO THE SCIENTIFIC DEGREE OF DOCTOR OF SCIENCE

To be granted the scientific degree of Doctor of Science (Ph. D.), the present Doctoral Thesis has been submitted for the defence at the open meeting of RTU Promotion Council on November 12, 2020 at 10:00 at the Faculty of Electrical and Environmental Engineering of Riga Technical University, 12/1 Azenes Street, Room 306.

OFFICIAL REVIEWERS

Lead researcher Dr. sc. ing. Romāns Petričenko
Riga Technical University, Institute of Power Engineering, Latvia

Professor Dr. sc. ing. Saulius Gudzius
Kaunas University of Technology, Lithuania

Principal Engineer Dr. sc. ing Andrejs Svalovs
General Electric, Switzerland

DECLARATION OF ACADEMIC INTEGRITY

I hereby declare that the Doctoral Thesis submitted for the review to Riga Technical University for the promotion to the scientific degree of Doctor of Science (Ph. D.) is my own. I confirm that this Doctoral Thesis has not been submitted to any other university for the promotion to a scientific degree.

Ivars Zālītis …….. (signature)

Date:……

The Doctoral Thesis has been written in English. It consists of an Introduction; 8 chapters; Conclusions; 85 figures; 25 tables; 3 appendices; the total number of pages is 179. The Bibliography contains 163 titles.

# TABLE OF CONTENTS

# INTRODUCTION

## The topicality of the subject of the Doctoral Thesis

Transmission lines are highly exposed to fault risk factors of environmental and anthropogenic nature. The fault statistics [1] confirm this as between 60 % and 70 % of faults in the high-voltage (hereafter – HV) grids of the Baltic region were transmission line faults. It can also be seen that on average 60.2 % and 67.6 % of these are phase-to-earth (hereafter – L-E) faults for 100–150 kV and 220–330 kV lines, respectively, in the Baltic region. These faults are known to result in poor performance of the many of existing distance protection (hereafter – DP) and fault location (hereafter – FL) algorithms that use the measurement data of only one terminal. This is due to the presence of the fault path resistance and fault current infeed from the other end of the line as well as the simplifications used for the model of the power system. One solution to this problem is application of communication networks between the substations. This allows implementing fast and accurate algorithms but they often require precise synchronisation of the measurement data. There is also a risk of communication loss due to the damage caused by the fault or for other reasons. Considering the above, it remains desirable to develop a method that could accurately determine the fault distance if the scope of information on the faulted line is limited to data, available at the "own" substation, at least as a backup to communication-related methods.

The fault statistics [1] also show that on average only 19.8 % and 29.5 % of the transmission line faults are permanent faults for 100–150 kV and 220–330 kV lines, respectively, in the Baltic region. Thus, in most cases, a transmission line can be successfully re-energised for operation after the deionisation of an electric arc channel at the fault point. As most of the faults involve one phase, it is usually possible to disconnect and reconnect only the faulted phase if separate control of the phase circuit breakers (hereafter – CB) is available. This is beneficial, as power transmission is retained via the healthy phases, resulting in less impact on the dynamic stability of the power system during the isolation of the fault and the reclosing procedure, especially in HV and extra-high-voltage networks. Often a conventional application of a fixed time setting determined based on the maximum possible deionisation time is still used. This can result in a larger impact on the system stability and a longer flow of undesirable zero-sequence (hereafter – ZS) current in the power transformer neutral line if the arc extinction is rapid. Therefore, it can be useful to obtain an adaptive single-phase automatic reclosing (hereafter – ASPAR) method.

## The hypothesis of the Doctoral Thesis

One-terminal-measurement-based approaches of FL and DP prove unreliable when a fault has a high transient resistance and the network topology is more complicated; such an approach can be replaced by a technique based on the estimation of unknown power system model parameters, solving the problem as an optimisation task with the aim to achieve independence from large-distance communication networks and better performance compared

with existing one-terminal-measurement-based methods. It is beneficial to divide this task into the estimation of pre-fault and fault regime parameters to decrease the number of unknown parameters for each particular stage. This method or its results can be used for other power system automation tasks.

## The aim of the Doctoral Thesis

The aim of the Doctoral Thesis is to develop a novel method of two-stage estimation of unknown power system model parameters and lay the foundation for the solution of FL, DP, ASPAR and similar problems via optimisation procedures, thus increasing the reliability and robustness of the power system.

## The tasks of the Doctoral Thesis

In order to achieve the aim of the Doctoral Thesis, the following tasks have been set.

1. Investigation of the performance of existing FL, DP and adaptive automatic reclosing methods and devices.
2. Description and development of modelling tools for pre-fault and fault regimes of the power system necessary for the implementation of the proposed method.
3. Creation of a framework for two-stage estimation of unknown power system model parameters.
4. Implementation of the created framework with optimisation tools for FL and DP.
5. Synthesis of an optimal objective function.
6. Testing of the developed FL and DP algorithms and comparison with existing methods.
7. Development of an adaptive single pole automatic reclosing algorithm, using the described modelling tools and the proposed model parameter estimation method.

## Methods and tools of research

The results presented in the Thesis were obtained by applying the following methods and tools.

1. Topological power system modelling methods.
2. The nodal potential (admittance) and the Gauss–Seidel method.
3. The symmetrical component method.
4. The model parameter estimation method.
5. The genetic algorithm.
6. Computations, simulations and data processing in MATLAB©, MATLAB SimPowerSystems©.
7. ISA DRTS 64 signal generator using waveform playback from COMTRADE files of ISA TDMS 7.0.4©.
8. High-voltage 110–220 kV transmission line protection terminal REDI.
9. Smoky, a program for reading fault recordings.

## The scientific novelty of the Doctoral Thesis

1. A novel numerical method of topological modelling of multiple simultaneous asymmetrical power system faults.
2. A novel method of hybrid (symmetrical components and per-phase integration) topological modelling of a HV line.
3. Two-stage optimisation-based estimation of unknown model parameters and its implementation for FL, DP and adaptive automatic reclosing.
4. Development of parameter selection strategies for the synthesis of an optimal objective function used by the proposed parameter estimation method.
5. Application of numerical inversion of the Laplace transform in conjunction with topological network analysis.
6. The technique of mixed virtual/real testing of a DP terminal in cases of faults with a non-stationary fault path resistance such as faults caused by fallen trees.

## The practical significance of the Doctoral Thesis

1. The proposed modelling methods can be used for future analysis and development of relay protection and automation.
2. The proposed method can be used as a basis for the development of highly robust FL and DP devices that are immune to fault path resistance and capable to operate without data communication.
3. The developed adaptive automatic reclosing algorithm can be implemented into a corresponding device, which would offer a significant contribution to system stability.

## Author's personal contribution to the research performed

The modelling methods for power system stationary and transient regimes as well as the framework for the model parameter estimation method were developed under the supervision of Associate Professor Aleksandrs Dolgicers. The literature analysis, modelling implementations into program codes, simulation and testing results, applications of the proposed method for the FL, DP, ASPAR, and the Conclusions belong personally to the author.

## Volume and structure of the Doctoral Thesis

The Doctoral Thesis is written in English. It comprises an introduction, 8 chapters with 34 sections, conclusions and a list of references with 163 cited sources of information. The Thesis contains 75 equations, 25 tables, 85 figures, and 3 appendices. The total volume of the Thesis is 179 pages, including appendices.

Chapter 1 describes interaction of external factors and control systems with the power system as a controlled object. The role of modelling and optimisation in power system control is also indicated. Next, simplifications used for control systems and the proposed method are

discussed and descriptions of power system control subtasks of FL, DP, and single-phase automatic reclosing (hereafter – SPAR) are given. Finally, description of an application of the proposed method for FL is introduced. Chapter 2 provides extensive technical background of FL and DP methods and devices as well as technical background of ASPAR. Chapter 3 describes general principles of modelling of stationary asymmetrical power system faults including both shunt and series (usually short circuits and open phase) faults according to the method of symmetrical components. The most commonly used complex equivalent circuits for these faults are also presented. Additionally, descriptions of two numerical calculation methods for multiple stationary simultaneous asymmetric faults are given. Chapter 4 is dedicated to mathematical methods suitable for the calculation of stationary pre-fault and fault regime state parameters on the basis of topological modelling, particularly the nodal potential (admittance) method in conjunction with the Gauss–Seidel method as a numerical solver. A numerical inverse Laplace transform in combination with topological analysis of the power system is also presented for calculation of the free component of transient current and voltage waveforms or for use in control systems with models in Laplace space. Additionally, the results of the testing of an existing DP terminal using a virtual-real laboratory for faults with non-stationary fault path resistance are presented. Chapter 5 includes a general framework of the proposed model parameter estimation method. Next, the implementations of different optimisation tools for FL and DP are demonstrated. The chapter also presents some of the results obtained by the initially used modified randomised search as the optimisation core. Chapter 6 presents the possible parameter selection strategies used to obtain an optimal objective function for the proposed method. In-depth analysis of objective function surfaces created by single parameters and the principles of their interaction that should minimise the presence of false extrema are presented. Chapter 7 is dedicated to the testing of the performance of the implementation of the proposed method with the genetic algorithm (hereafter – GA) for FL. After a description of the case study network, parameter groups obtained by the conservative and opportunistic strategies described in Chapter 6 are presented. Chapter 7 also shows the effects of using different parameter group sizes and selection strategies on the surfaces of the objective function. Then, the results and analysis of an extensive testing of the FL using the proposed method and a comparison with existing one-terminal- and two-terminal-measurement-based FL methods are given. Chapter 8 demonstrates an approach to detailed modelling of a transmission line during the dead time of SPAR. The described approach is used to analyse the changes of line-side faulted phase voltage during the dead time for various fault distances and equivalent fault path resistances. Next, dynamic arc models are implemented to represent the nonlinear character of both the primary and secondary arc and the elongation as well as the extinction of the fault secondary arc. Based on the analysis of both steady-state and dynamic simulation results, an ASPAR algorithm with a dedicated logic block was developed and tested in scenarios of transient faults with different fault arc elongation speeds and permanent faults. Finally, the main results of the Thesis are summarised in Conclusions.

## Approbation of the Doctoral Thesis

The results of the research have been presented at international scientific conferences in Latvia and abroad.

1. The 4th Workshop on Advances in Information, Electronic and Electrical Engineering (AIEEE'2016), Vilnius, Lithuania, 10–12 November 2016.
2. 2017 17th IEEE International Conference on Environment and Electrical Engineering and 2017 IEEE Industrial and Commercial Power System Europe (EEEIC / I&CPS Europe), Milan, Italy, 6–9 June 2017.
3. 12th IEEE PES Powertech Conference Towards and Beyond Sustainable Energy Systems, Manchester, United Kingdom, 18–22 June 2017.
4. 2017 IEEE 58th International Scientific Conference on Power and Electrical Engineering of Riga Technical University (RTUCON 2017), Riga, Latvia, 12–13 October 2017.
5. The 5th Workshop on Advances in Information, Electronic and Electrical Engineering (AIEEE'2017), Riga, Latvia, 24–25 November 2017.
6. The 6th IEEE Workshop on Advances in Information, Electronic and Electrical Engineering (AIEEE'2018), Vilnius, Lithuania, 8–10 November 2018.

The results of the research have been published in the proceedings of scientific conferences and a scientific journal.

1. A. Dolgicers, **I. Zalitis**, and J. Kozadajevs. The Modified Seidel Method as a Tool for the Evaluation of the Stability of a Power System. In: *2016 IEEE 4th Workshop on Advances in Information, Electronic and Electrical Engineering (AIEEE'2016)*, Vilnius, Lithuania, 10–12 November 2016. Piscataway: IEEE, 2017, pp. 27–33, ISBN: 978-1-5090-4474-0. Available from: DOI: 10.1109/AIEEE.2016.7821806.
2. **I. Zalitis**, A. Dolgicers, and J. Kozadajevs. A power transmission line fault locator based on the estimation of system model parameters. In: *Proceedings 2017 IEEE International Conference on Environment and Electrical Engineering*, Milan, Italy, 6–9 June 2017. Piscataway: IEEE, 2017, pp. 1–6, ISBN: 978-1-5386-3918-4. Available from: DOI: 10.1109/EEEIC.2017.7977459.
3. **I. Zalitis**, A. Dolgicers, and J. Kozadajevs. A distance protection based on the estimation of system model parameters. In: *Proceedings 2017 IEEE Manchester PowerTech*, Manchester, UK, 18–22 June 2017. Piscataway: IEEE, 2017, pp. 1–6, ISBN: 978-1-5090-4238-8. Available from: DOI: 10.1109/PTC.2017.7981277.
4. A. Dolgicers and **I. Zalitis**. Numerical calculation method for symmetrical component analysis of multiple simultaneous asymmetrical faults. In: *Proceedings 2017 IEEE 58th International Scientific Conference on Power and Electrical Engineering of Riga Technical University*, Riga, Latvia, 12–13 October 2017. Piscataway: IEEE, 2017, pp. 1–7, ISBN: 978-1-5386-3847-7. Available from: DOI: 10.1109/RTUCON. 2017.8124748.

5. **I. Zalitis**, A. Dolgicers, and J. Kozadajevs. Experimental testing of distance protection performance in transient fault path resistance environment. In: *Proceedings 2017 5th IEEE Workshop on Advances in Information, Electronic and Electrical Engineering*, Riga, Latvia, 24–25 November 2017. Piscataway: IEEE, 2018, pp. 1–6, ISBN: 978-1-5386-4138-5. Available from: DOI: 10.1109/AIEEE.2017.8270526.
6. **I. Zalitis**, A. Dolgicers, and J. Kozadajevs. Influence Analysis of Mutual Coupling Effects between a High-Voltage Transmission Line and a Fiber-optic Cable with a Conductive Support Element. In: *2018 IEEE 6th Workshop on Advances in Information, Electronic and Electrical Engineering (AIEEE'2018)*, Vilnius, Lithuania, 8–10 November 2018. Piscataway: IEEE, 2018, pp. 1–7, ISBN: 978-1-7281-2000-3. Available from: DOI: 10.1109/AIEEE.2018.8592447.
7. **I. Zalitis**, A. Dolgicers, and J. Kozadajevs. An adaptive single-pole automatic reclosing method for uncompensated high-voltage transmission lines. *Electric Power Systems Research*, vol. 166, Jan. 2019, pp. 210–222. ISSN: 0378-7796. Available from: https://doi.org/10.1016/j.epsr.2018.10.012.

One patent has been obtained.

1. Riga Technical University. *Transmission line single-phase-to-ground fault locator method*. A. Dolgicers, **I. Zalitis,** J. Kozadajevs (inventors). Int. Cl.: H02H7/26. LV Patent 15207, issued May 20, 2017. 20 p. Available from: https://worldwide.espacenet.com/publicationDetails/originalDocument?FT=D&date=20170520&DB=&locale=en_EP&CC=LV&NR=15207B&KC=B&ND=4#.

# 1. FAULT LOCATION, DISTANCE PROTECTION AND ADAPTIVE AUTOMATIC RECLOSING AS PARTS OF THE POWER SYSTEM CONTROL

## 1.1. Mathematical Statement of the Protective Automation Problem

Power system operation is affected by parameters of the systems elements $\boldsymbol{P}(t)$ (electrical impedances, admittances), external known parameters $\boldsymbol{X}(t)$ (current electricity price, temperature), external partially predictable stochastic parameters $\boldsymbol{S}(t)$ such as faults and control processes $\boldsymbol{C}(t)$ (transformer, generator voltage regulation). These determine controlled state parameters $\boldsymbol{Y}(t)$ (node voltages, branch currents). Both $\boldsymbol{X}(t)$ and $\boldsymbol{Y}(t)$ are determined with errors $\varepsilon(t)$. Based on available data a control system has to perform control operations, which ensure optimal operation of the power system, adherence to imposed limitations of $\boldsymbol{Y}(t)$, and provide necessary information $\boldsymbol{I}(t)$ about the power system to the personnel [2]–[6]. Sometimes due to lack of measurement data or external influences the control system might be required to estimate real $\boldsymbol{P}(t)$ and/or $\boldsymbol{S}(t)$ or unavailable state parameters $\boldsymbol{Y}(t)$. This can be achieved using optimisation tools, which diminish the difference between the model output $\boldsymbol{Y}_{\mathbf{M}}(t)$ and corresponding available measurements $\boldsymbol{Y}(t)$ from the real power system (Fig. 1.1) or estimate part of these parameters and replace others with probability distributions [7], [8].

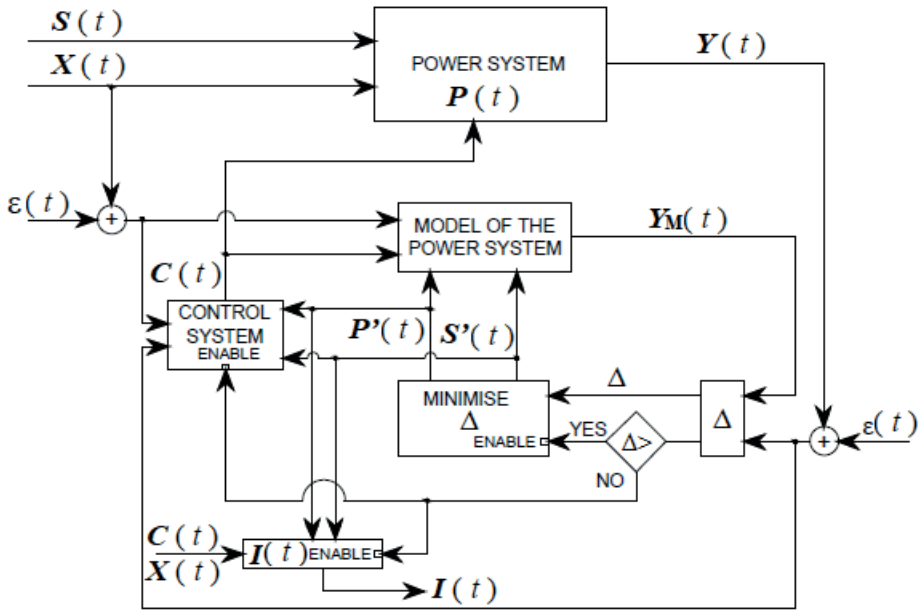


Fig. 1.1. Closed-loop control system incorporating an estimation of unknown system paramters $\boldsymbol{P}(t)$ and stochastic external processes $\boldsymbol{S}(t)$ with an optimisation tool.

The whole control system problem is nonlinear, stochastic, and multi-criterial and includes many state and optimisation variables, and as such this problem cannot be solved without some simplifications. In this Thesis, only part of the control system – protective automation – will be considered with particular focus on the FL, DP, and AR created by applying the parameter estimation. Models used for parameter estimation will be lumped and linear and only the fundamental harmonic components of the measured signals will be

considered. Measurement errors will be disregarded when testing both the proposed method and existing methods for comparison so that errors arise only from the deficiencies or limitations of the methods themselves.

## 1.2. Fault Location, Distance Protection and Automatic Reclosing Functions

As this Thesis focuses on FL, DP and AR methods for overhead transmission lines (hereafter – OHTL), a brief description of these functions will be given.

The main task of FL methods is estimation of distance α from the substation of the FL device to the fault [9], [10]. The main requirement to the FL is accuracy, as it reduces the time necessary for the identification and the repair of the fault resulting in improved resilience of the power system.

DP is closely related to FL, as one of main operations it has to perform is to estimate the fault distance, which is expressed as an apparent impedance determined by a DP relay $Z_{rel} = f(\alpha)$. In most cases it is calculated using faulted phase busbar voltages and current measurements from one substation. The primary task of DP is to determine the presence of a fault in the protected OHTL based on $Z_{rel}$ and clear it by opening the controlled CB. The main requirements of DP are operation speed, sensitivity (capability to operate for all faults in elements protected by DP at most unfavourable operation conditions), and selectivity (capability to operate only for intended fault scenarios, prioritising protection devices that are closest to the fault) [5], [11]–[14].

The main task of AR is to re-energise the line for some time called “dead time” after the clearing of the fault and then reconnect it if the fault has been transient in nature. The main requirement of AR is to minimise the dead time necessary before the reclosing, because during this time power system resilience is decreased, while retaining sufficient time for restoration of insulation strength. In cases of L-E faults an AR subtype disconnecting and reclosing only one phase – SPAR – can be used. In this Thesis a further subtype of SPAR that changes the dead time setting – ASPAR – will be considered [3], [4], [6], [14].

## 1.3. The General Approach of the Proposed Method

The estimation of unknown power system fault parameters is achieved by applying optimisation that is further supplemented, first, by an additional estimation of pre-fault parameters of the system. This increases the information available before the estimation of system model parameters for the fault regime (operation mode). Secondly, in contrast to two-terminal-measurement-based methods, the proposed method extends available measurement scope to other system elements within the controlled substation rather than from the other end of the line. To accommodate the increased measurement scope, the models used must exceed the two-machine network or an isolated model of the line that is often applied [15], [16].

## 1.4. Conclusions

1. FL, DP and AR are subtasks of a more general problem – power system control – that aims to sustain and optimise the operation of the system.
2. Some of the automation and protection functions may solve the lack-of-information problem elements due to lack of measurement data or changes of the system caused by external influences such as faults via estimation of unknown parameters of the power system.
3. The main task of the FL is estimation of the fault distance from the substation, and the main requirement is accuracy in terms of line length.
4. DP is used to clear faults in power system elements it protects by opening the CB it controls. The most important requirements to DP are operation speed, sensitivity to ensure intended operation even in unfavourable fault scenarios and selectivity to restrain from premature or unintended operation.
5. The main task of AR is to re-energise a transmission line after a fault in it is cleared and reconnect the second end of the line if the fault has been transient in nature.
6. The main requirement to AR is the minimisation of the time before the line is re-energised and reconnected while ensuring restoration of insulation strength at the fault point.

# 2. TECHNICAL BACKGROUND OF FAULT LOCATION, DISTANCE PROTECTION AND ADAPTIVE AUTOMATIC RECLOSING METHODS

## 2.1. Existing Fault Location Methods

One of the first approaches to FL were topological or inspection methods, the simplest one being sectionalisation of the OHTL with disconnection switches [17]. By 1949, fault indicators (hereafter – FI) installed on line towers were invented, starting from a gunpowder cartridge fuse that releases a mechanical indicator [18], [19] to electromagnetic FI with automatic resetting [20]. In 1989, using fibre optic communication with FI to determine the faulted line section was proposed [21]. Today, FI are more often used in distribution networks and more research is dedicated to optimal placement of FI [22], [23]. Another inspection-based FL method used a tracer signal of the fifth harmonic with a mobile sensor [18], [19]. Similar approaches are used today in power cable networks [24]. In most cases, these methods are time-consuming, especially in hard-to-access terrain, and require investments for additional equipment.

The second group uses transient waves of current or voltage, usually referred to as the travelling wave (hereafter – TW) method. TW method applications have been reported since 1931 [25]. Initially, these methods used recordings of oscilloscopes [26]–[28]. Several types of TW FL were developed in this time period: type A, which measures the time necessary for the first voltage collapse wave reflection to return to the substation; type B, which used the time difference between wave arrivals at both ends of the line; types C and F, which are pulse radar methods using direct current (hereafter – DC) or radio-frequency pulses; and type D, which is similar to type B but the measurements are performed by synchronised timers [18], [19], [27], [28]. By 1985, TW FL were applied to HV direct current lines by measuring the time between the arrival of the first and the next wave of the same polarity as the first one [29], [30]. After that, in 1996, it was proposed to combine TW FL with the global positioning system (hereafter – GPS) for time-stamping [31], and by 1998 and 1999, use of artificial neural networks (hereafter – ANN) with the Prony method and continuous wavelet transformation was proposed for signal processing of TW FL [32], [33]. Recently, the research of this type of FL has been targeting specific fault and line types [34], [35]. The reported accuracy of TW FL is typically within one tower span or does not exceed 1 %, but it should be mentioned that most TW methods require high time resolution, which can make the FL equipment expensive, and well-tuned correlation blocks to avoid errors due to additional wave fronts and wave decay.

The next group of FL methods use electrical measurements (most often steady-state quantities of the fault regime) with a model of the line to determine the fault distance. Initially, the measurements were carried out after de-energising the line by connecting an external DC source or an alternating current (hereafter – AC) generator with a step-up transformer [17]. The next approach used fault regime measurement recordings and pre-calculated curves of faulted and/or healthy parallel line currents for FL [18], [19], [36], [37].

Starting around the 1980s, digital applications using Thevenin's equivalents of one or both ends of the line were developed. These developed nonlinear equation systems from Kirchhoff's laws [38], determined fault distance based on DP apparent reactance [15] or applied superimposed components of measurements [16], [39]. Later, two-terminal-measurement based FLs were developed, initially using manual measurement acquisition [40], but later both GPS and phasor measuring units were introduced for data exchange [41]–[43]. Modification of the discrete Fourier transform for signal processing was also applied in these papers. Since 1996, ANN has been applied for FL by using several frequency ranges of instantaneous voltage and current signals [44]. Later, ANN was combined with other intelligent algorithms to add functions of fault type identification and selection of the optimal FL method [45], [46]. Various optimisation approaches are also known, such as minimisation of the difference between fault point voltages calculated separately from two-terminal measurements [47] and substitution of remote-end power system equivalent impedance with a probability distribution while using the Monte-Carlo method, which tests if the imaginary part of the apparent power at the fault point is equal to zero [7], [8]. Later, approaches similar to [47], but implemented with the GA and then Whale optimisation were also presented [48]–[50]. The initial approaches using pre-calculated curves had errors up to 20 % due to measurement errors and the low quality of the curves used. The digital implementations with Thevenin's equivalents could not often fully compensate for errors due to the limited scope of information due to the model simplifications or assumptions used. ANN is a versatile tool but it requires a training data base (possibly for each substation or relay). The two-terminal-measurement-based FL methods are fast and accurate but they require secure and well-synchronised communication networks, which can be compromised due to the fault or other reasons. The optimisation approaches often result in higher computation cost, which is less critical to FL compared with, say, relay protection.

Considering the possibility of loss of communications between the substations during the fault and the aforementioned drawbacks of FL methods using one-terminal measurements, it was concluded that an algorithm capable of solving the FL task in this incomplete information environment would prove beneficial.

## 2.2. Existing Distance Protection Methods

The early development of DP in the 1920s and 1930s started with the so-called balanced-beam-type DP relay but the first practical implementations, known as C-Z type DP relays, consisted in combination with the induction disc overcurrent relay [51]–[56]. By 1930, the stepped coordination principle for selectivity was introduced, the first descriptions of the influence of fault path resistance were given, the reactance DP relay was proposed and research on electronic DP had begun [57]. Later, compensation of the voltage drop caused by ZS current for the faulted line and a healthy parallel line was introduced for both C-Z and reactance-type DP relays [58], [59].

The 1940s saw application of selector relays to decrease the total cost of DP relaying systems [60]. As three-terminal lines became more common at that time, DP setting strategies

and a combination with carrier-pilot communication was developed for these lines [61]. A DP relay proposed in 1944 provided, for the first time, the opportunity to move and shift the operation region in the complex impedance plane [62], which greatly facilitated DP coordination. This period also saw development of the analysis of power swing influence on apparent impedance and the operation of DP [63], [64].

During the 1950s and 1960s, practical electronic and later transistor-based DP relays were developed, implemented with either coincidence circuits or other phase comparison blocks [65], [66]. Development of electromechanical relays resulted in a combined DP relay for all phase-to-phase (hereafter – L-L), phase-to-phase-to-earth (hereafter – L-L-E) faults [67], [68]. By 1966, the first approximation of a quadrilateral DP operation region was created in an electronic DP relay [69].

The 1970s saw several improvements in electronic DP relays using the quadrilateral operation region [70], [71]. Starting from 1971, papers proposing microprocessor-based DP were published that included implementations of DP logic and development of signal processing techniques [72]–[74], [75], [76]. Versions of a combined electronic DP relay for all asymmetrical faults based on the phase sequence of ZS compensated L-E voltages were also developed [77], [78]. In 1977, possibly the first paper considering online adaptation of the DP operation region based on pre-fault power flow was published [79], which is one of the few approaches considering pre-fault regime in the DP itself.

In the time period of the 1980s and 1990s, an application of TW FL that determined fault distance for the DP was proposed [80]. A modification of DP using only negative-sequence (hereafter – NS) and ZS currents and voltages was also presented [81]. This time period also saw increased interest in the adaptive operation region approach, either proposing additional reactance setting compensation due to frequency deviations [82] or by implementing an approximation of the full adaptive operation region (considers all the possible $Z_{rel}$ for a given pre-fault power flow) [83]. Several directional elements for DP based on superimposed components were also introduced during this period [84], [85]. A 1996 paper was one of the first to introduce ANN for DP adaptive DC offset and Fourier filters [86]. Some papers focused on DP coordination strategies based on either coordination rules [87] or probabilistic approaches using statistical data and simulations [88]. A 1999 paper proposed minimising the difference between measured voltage samples and the ones calculated from current measurements and line differential equations [89].

Lastly, some of the DP versions proposed since the year 2000 will be mentioned. This period also saw new versions of the adaptive operation region approach, such as ANN-based implementation [90] and separation into a fixed part and an adaptive one obtained using the supervisory control and data acquisition system [91]. Some papers performed a more in-depth analysis of the influence of signal distortions on the performance of DP [92], [93]. A Monte-Carlo-method-based approach similar to the one mentioned in FL analysis was also developed for DP [94]. A 2011 paper proposed determining optimal DP settings by minimising the sum of the probabilities of losing selectivity and sensitivity weighted by a priority coefficient [95]. Starting from 2015, papers dedicated to DP for parallel OHTL L-E and cross-country faults (one faulted phase in each line) were published [96], [97]. A topic that has lately attracted

significant researchers' interest is development of better DP blocking methods and possible correct operation of DP during power swings [98]–[100].

From the foregoing analysis, it can be seen that the initial development of DP was oriented towards achieving cheaper and more practical DP relaying for both phase and earth faults. The pre-fault power flow and fault path resistance was mainly considered with extension of static settings. A similar trend continued as the same DP principles were implemented in electronic-based devices. The introduction of microprocessors provided opportunities for better signal processing approaches, but it was only starting from 1977 with the advent of adaptive DP operation regions that the DP itself could consider pre-fault power flow. Besides modifications of the adaptive operation region approach, the main attempts to consider remote-end infeed consisted in the use of current distribution coefficients, which often involved additional assumptions, implementation that avoided the use of positive-sequence (hereafter – PS) quantities of relay voltage, current and optimisation approaches.

## 2.3. Existing Adaptive Single-Pole Automatic Reclosing Methods

Wide-spread interest and development of ASPAR can be observed since the 1990s. Several ASPAR methods were provided in [101], starting from the use of the absolute value of faulted phase voltage (about 0.5–1.0 p.u. after the complete arc deionisation if the compensation coefficient for PS capacitance was above 0.7 p.u.). This method is unsuitable for partially compensated or uncompensated OHTLs, and using the angle between the faulted phase voltage and the ZS current is proposed for such lines. The third method intended for partially compensated lines (the compensation coefficient being below 0.6 p.u.) is control of the period of the faulted phase voltage [101]; however, the performance of this method may be affected by fluctuations of power frequency caused by other reasons. An approach comparing a measured voltage signal with a modelled voltage sine signal with a DC offset [102] is also known, which would require a high sampling frequency. ANNs using the DC component and the 1st–4th harmonic components of measurement recordings for training have also been used for ASPAR [103]. Another method proposed determining the time of arc extinction by an abrupt change in the faulted phase voltage root mean square (hereafter – RMS) value [104]. The next method identifies two events of a voltage drop (the outset of the fault and the disconnection of the CBs) followed by a voltage increase (the secondary arc has been quenched) [105]. This approach may fail if the fault with a small fault path resistance occurs close to the substation. Using the presence of a voltage DC component was also proposed to determine the moment when the fault arc has been extinguished [106] but a significant DC component surge is also present after the disconnection of the CBs. Other methods developed specifically for compensated lines based on the harmonic composition of the currents of shunt reactors are also known [107], [108].

## 2.4. Conclusions

1. Measurements from both terminals of the line provide opportunities for fast and accurate FL but their operation can be critically affected in case of loss of communication between substations or loss of synchronisation of these measurements.
2. Existing FL methods using one-terminal measurements utilise algorithms that are independent from the influence of the remote-end infeed such as TW methods, or approximate this influence by using methods such as ANN and Monte-Carlo.
3. Most of the research on DP was more oriented towards various implementations of the DP itself in electromechanical, electronic or digital devices.
4. The loss of sensitivity due to the remote-end infeed can be partially compensated with adaptive DP operation regions, but this increases the risk of loss of selectivity.
5. Some of the existing ASPAR methods control changes in the value of faulted phase voltage or try to detect the presence of either voltage signal distortions or DC offset. Others are developed specifically for lines with shunt reactors and these methods operate based on resulting higher-harmonic components of either voltage or current signals.
6. Most ASPAR methods ignore the influence of healthy-phase power flow or they are highly dependent on accurate measurements of higher-harmonic components or DC offset, requiring a higher sampling frequency and resulting in more expensive devices.

# 3. MODELLING OF ASYMMETRICAL REGIMES OF A POWER SYSTEM

## 3.1. A Single Transverse Asymmetry

The power system points where a single transverse asymmetry is present can be represented with different phase shunt impedances and a common neutral impedance to earth, which can be used with the symmetrical component operator $\dot{a} = \mathrm{e}^{i120^\circ}$ to link symmetrical components of the calculation phase fault voltage to the symmetrical components of the phase fault current:

$$\begin{cases} \dot{U}^1_{\mathrm{KA}} = \frac{1}{3}[\dot{I}^1_{\mathrm{KA}}(\dot{Z}_{\mathrm{KA}} + \dot{Z}_{\mathrm{KB}} + \dot{Z}_{\mathrm{KC}}) + \dot{I}^2_{\mathrm{KA}}(\dot{Z}_{\mathrm{KA}} + \dot{a}^2\dot{Z}_{\mathrm{KB}} + \dot{a}\dot{Z}_{\mathrm{KC}}) \\ \dot{U}^2_{\mathrm{KA}} = \frac{1}{3}[\dot{I}^1_{\mathrm{KA}}(\dot{Z}_{\mathrm{KA}} + \dot{a}\dot{Z}_{\mathrm{KB}} + \dot{a}^2\dot{Z}_{\mathrm{KC}}) + \dot{I}^2_{\mathrm{KA}}(\dot{Z}_{\mathrm{KA}} + \dot{Z}_{\mathrm{KB}} + \dot{Z}_{\mathrm{KC}}) \\ \dot{U}^0_{\mathrm{KA}} = \frac{1}{3}[\dot{I}^1_{\mathrm{KA}}(\dot{Z}_{\mathrm{KA}} + \dot{a}^2\dot{Z}_{\mathrm{KB}} + \dot{a}\dot{Z}_{\mathrm{KC}}) + \dot{I}^2_{\mathrm{KA}}(\dot{Z}_{\mathrm{KA}} + \dot{a}\dot{Z}_{\mathrm{KB}} + \dot{a}^2\dot{Z}_{\mathrm{KC}}) \\ \qquad + \dot{I}^0_{\mathrm{KA}}(\dot{Z}_{\mathrm{KA}} + \dot{a}\dot{Z}_{\mathrm{KB}} + \dot{a}^2\dot{Z}_{\mathrm{KC}})], \\ \qquad + \dot{I}^0_{\mathrm{KA}}(\dot{Z}_{\mathrm{KA}} + \dot{a}^2\dot{Z}_{\mathrm{KB}} + \dot{a}\dot{Z}_{\mathrm{KC}})], \\ \qquad + \dot{I}^0_{\mathrm{KA}}(\dot{Z}_{\mathrm{KA}} + \dot{Z}_{\mathrm{KB}} + \dot{Z}_{\mathrm{KC}} + 9\dot{Z}_{\mathrm{KN}})], \end{cases} \tag{3.1}$$

where $\dot{U}^1_{\mathrm{KA}}$, $\dot{U}^2_{\mathrm{KA}}$, $\dot{U}^0_{\mathrm{KA}}$ – phasors of PS, NS and ZS quantities of Phase A voltage at the fault point, V;

$\dot{I}^1_{\mathrm{KA}}$, $\dot{I}^2_{\mathrm{KA}}$, $\dot{I}^0_{\mathrm{KA}}$ – phasors of PS, NS and ZS quantities of Phase A current at the fault point, A;

$\dot{Z}_{\mathrm{KA}}$, $\dot{Z}_{\mathrm{KB}}$, $\dot{Z}_{\mathrm{KC}}$ – fault impedances of Phase A, Phase B and Phase C, Ω;

$\dot{Z}_{\mathrm{KN}}$ – the neutral impedance at the fault point, Ω.

The equation system (3.1) can be used in combination with separate sequence networks for a numerical steady-state calculation similar to [109] by representing the symmetrical components of the fault point voltage $\dot{U}^1_{\mathrm{KA}}$, $\dot{U}^2_{\mathrm{KA}}$, $\dot{U}^0_{\mathrm{KA}}$ with electromotive force (hereafter – EMF) sources. This approach can also be used for general transverse asymmetry ($0 \leq \dot{Z}_{\mathrm{KA}} \neq \dot{Z}_{\mathrm{KB}} \neq \dot{Z}_{\mathrm{KC}} < \infty$ Ω), but if the fault path impedances of at least two phases are equal, it is possible to use complex equivalent circuits with electrical interconnections between sequence networks [110]. These are numerically more stable than the use of separate sequence networks and convenient for the proposed method as they provide symmetrical components for all branch currents and node voltages from a single regime calculation.

## 3.2. A Single Longitudinal Asymmetry

A single longitudinal asymmetry can be represented by series impedances in phases, which can be used to link the symmetrical components of the special phase voltage drop and the symmetrical components of the special phase current:

$$\begin{cases} \Delta\dot{U}^1_{\mathrm{LA}} = \frac{1}{3}[\dot{I}^1_{\mathrm{LA}}(\dot{Z}_{\mathrm{LA}} + \dot{Z}_{\mathrm{LB}} + \dot{Z}_{\mathrm{LC}}) + \dot{I}^2_{\mathrm{LA}}(\dot{Z}_{\mathrm{LA}} + \dot{a}^2\dot{Z}_{\mathrm{LB}} + \dot{a}\dot{Z}_{\mathrm{LC}}) \\ \Delta\dot{U}^2_{\mathrm{LA}} = \frac{1}{3}[\dot{I}^1_{\mathrm{LA}}(\dot{Z}_{\mathrm{LA}} + \dot{a}\dot{Z}_{\mathrm{LB}} + \dot{a}^2\dot{Z}_{\mathrm{LC}}) + \dot{I}^2_{\mathrm{LA}}(\dot{Z}_{\mathrm{LA}} + \dot{Z}_{\mathrm{LB}} + \dot{Z}_{\mathrm{LC}}) \\ \Delta\dot{U}^0_{\mathrm{LA}} = \frac{1}{3}[\dot{I}^1_{\mathrm{LA}}(\dot{Z}_{\mathrm{LA}} + \dot{a}^2\dot{Z}_{\mathrm{LB}} + \dot{a}\dot{Z}_{\mathrm{LC}}) + \dot{I}^2_{\mathrm{LA}}(\dot{Z}_{\mathrm{LA}} + \dot{a}\dot{Z}_{\mathrm{LB}} + \dot{a}^2\dot{Z}_{\mathrm{LC}}) \end{cases}$$

$$\begin{aligned} &+\dot{I}^0_{\mathrm{LA}}(\dot{Z}_{\mathrm{LA}} + \dot{a}\dot{Z}_{\mathrm{LB}} + \dot{a}^2\dot{Z}_{\mathrm{LC}})], \\ &+\dot{I}^0_{\mathrm{LA}}(\dot{Z}_{\mathrm{LA}} + \dot{a}^2\dot{Z}_{\mathrm{LB}} + \dot{a}\dot{Z}_{\mathrm{LC}})], \\ &+\dot{I}^0_{\mathrm{LA}}(\dot{Z}_{\mathrm{LA}} + \dot{Z}_{\mathrm{LB}} + \dot{Z}_{\mathrm{LC}})], \end{aligned} \tag{3.2}$$

where $\Delta\dot{U}^1_{\mathrm{LA}}$, $\Delta\dot{U}^2_{\mathrm{LA}}$, $\Delta\dot{U}^0_{\mathrm{LA}}$ – phasors of PS, NS and ZS quantities of Phase A voltage drop at the fault point, V;

$\dot{I}^1_{\mathrm{LA}}$, $\dot{I}^2_{\mathrm{LA}}$, $\dot{I}^0_{\mathrm{LA}}$ – phasors of PS, NS and ZS quantities of Phase A current at the fault point, A;

$\dot{Z}_{\mathrm{LA}}$, $\dot{Z}_{\mathrm{LB}}$, $\dot{Z}_{\mathrm{LC}}$ – fault impedances of Phase A, Phase B and Phase C, Ω.

The equation system (3.2) can be used with separate sequence networks in a numerical regime calculation process that is similar to the one described for a single transverse asymmetry. This approach can also be used for the analysis of general longitudinal asymmetry ($0 \leq \dot{Z}_{\mathrm{LA}} \neq \dot{Z}_{\mathrm{LB}} \neq \dot{Z}_{\mathrm{LC}} < \infty$ Ω), but if two series phase impedances are identical, it is possible [110] and recommended (for the reasons mentioned in Section 3.1) to use complex equivalent circuits.

## 3.3. Multiple Simultaneous Asymmetries

Regimes with multiple asymmetries present are either short circuits, which have triggered overvoltages that in turn caused other short circuits, combinations of short circuits and open phase "faults" (during the operation of SPAR), etc. In this Thesis, the main application for the calculation approaches used for simultaneous asymmetries is determination of the regime of healthy phases during ASPAR necessary for detailed modelling of the line in phase coordinates (see Chapter 8). In theory, complex equivalent circuits can be applied for most simultaneous asymmetries only if ideal transformers that are hard to accurately represent are used [110], [111], [112]. The author of [111] proposed replacing ideal transformers with adaptable EMF sources that enforce the boundary conditions, but did not present any practical implementations. Two different numerical adaptations were developed based on this technique by the author for the calculation of the power system regimes with multiple simultaneous asymmetries.

The first adaptation uses one complex equivalent circuit or one set of sequence networks. If possible, one of the asymmetries is represented with direct electrical interconnections while other asymmetries are considered by additional EMF sources updated during the numerical calculation process according to the equation systems (3.1) and/or (3.2). When all of the asymmetries are general, one set of sequence networks is used and all of the asymmetries are represented with EMF sources updated as described in Section 3.1, but this approach is numerically less stable than the use of direct interconnections of a complex equivalent circuit.

The second adaptation requires that one complex equivalent circuit where one of the asymmetries is represented with direct electrical interconnections should be created for every asymmetry. This is because the added EMF sources representing other asymmetries are updated using voltage drops from equivalent circuits where they are represented with direct interconnections [109]. This approach was numerically stable even when the values of fault path or series impedances of phases were significant.

In the face of intended extension of measurement scope used for the proposed method as described in Section 1.3, application of topological modelling methods for extended equivalent circuits of the power system that could calculate currents and voltages of multiple power system elements simultaneously would be desirable. The symmetrical-component-based modelling approaches described in this chapter still require a mathematical description for the equivalent circuits and numerical solution methods for their solution, which will be provided in Chapter 4.

## 3.4. Conclusions

1. Asymmetrical regimes of the power system, which include most common faults, can be numerically modelled using the symmetrical component method.
2. Regime calculation for a single point of asymmetry can be performed by iteratively recalculating the values of the EMF sources representing the asymmetry in separate sequence networks according to the boundary conditions of this asymmetry or by using one complex equivalent circuit if at least two phases have the same impedance at the point of the asymmetry.
3. Fault regimes with multiple simultaneous asymmetries can be modelled by one complex equivalent circuit with electrical interconnections representing one of the asymmetries and iteratively recalculated EMF sources representing the other asymmetries or by interchanging calculation of regimes for two or more of such complex equivalent circuits where each circuit represents a different asymmetry with electrical interconnections.

# 4. APPLICATIONS OF TOPOLOGICAL METHODS FOR MODELLING OF POWER SYSTEM REGIMES

## 4.1. Nodal Potential Method in Matrix Form

In order to calculate the currents and voltages of the power system necessary for further analysis, one can manually compose equations according to Kirchhoff's and Ohm's laws applied to an equivalent circuit and solve them [113], [114], yet considering the necessity to integrate this calculation process into an optimisation, a more computer-friendly topological nodal potential (admittance) method in matrix form was chosen. The equation system of the nodal potential method in matrix form is as follows [115]:

$$Y\boldsymbol{U} = \boldsymbol{I} - MZ^{-1}\boldsymbol{E} + \boldsymbol{Y}_{\mathrm{B}}U_{\mathrm{B}}, \tag{4.1}$$

where $Y$ – the matrix of the nodal admittances ($Y = MZ^{-1}M^{\mathrm{T}}$), s;

$\boldsymbol{U}$ – the vector of the node voltages, V;

$\boldsymbol{I}$ – the vector of the current sources, A;

$M$ – the first-incidence matrix of the network topology graph;

$Z$ – the matrix of the network impedances, Ω;

$\boldsymbol{E}$ – the vector of the branch EMFs, V;

$\boldsymbol{Y}_{\mathrm{B}}$ – the base node admittance vector, s;

$U_{\mathrm{B}}$ – the base node voltage, V.

In order to obtain the unknown node voltages, one must then solve the linear equation system (4.1), which can be done in multiple ways: by Cramer's rule, factorisation, etc. In this Thesis, either the inbuilt Gauss solver of the simulation environment or the Gauss–Seidel method will be used.

## 4.2. Modelling of Steady-State Fault Regimes

When modelling the steady-state fault regimes, it will be assumed that the base node is earthed ($U_{\mathrm{B}} = 0$ V). The numerical solution of the resulting simplified equation system can be obtained by implementing the Gauss–Seidel method [115]:

$$\boldsymbol{U}_i^{k+1} = \sum_{j=1}^{i-1} C_{ij}\boldsymbol{U}_j^{k+1} + \sum_{m=i+1}^{n} C_{im}\boldsymbol{U}_m^{k} + \boldsymbol{D}_i, \tag{4.2}$$

where $n$ – the number of nodes in the equivalent circuit except the base node;

$k$ – the number of the approximation step of the Gauss–Seidel method;

$C$ – a coefficient matrix obtained from the matrix of nodal admittances ($C_{ij} = -Y_{ij}/Y_{ii}$, $C_{ii} = 0$);

$\boldsymbol{D}$ – a vector obtained from the matrix of nodal admittances and the vector of constant terms ($\boldsymbol{B} = \boldsymbol{I} - MZ^{-1}\boldsymbol{E}$, $\boldsymbol{D}_i = -\boldsymbol{B}_i/Y_{ii}$).

The implementation of (4.2) is repeated for all nodes $i = 1, \ldots, n$ until the maximum difference between the node voltages of approximation step $k + 1$ and step $k$ has been reduced

below an accuracy setting ε chosen by the user (while $\varepsilon \leq \max_i\left(\left|\boldsymbol{U}_i^{k+1} - \boldsymbol{U}_i^{k}\right|\right)$). Then, the branch currents can be calculated by Ohm's law in matrix form [115]

$$\boldsymbol{I}_\mathrm{Z} = Z^{-1}[\boldsymbol{E} + M^\mathrm{T}(\boldsymbol{U} - U_\mathrm{B})], \tag{4.3}$$

where the values of the EMFs (vector $\boldsymbol{E}$) and the node voltages used are L-E values.

It is easy to see that the topological modelling technique combined with the nodal potential method in the matrix form and the use of complex equivalent circuits provides a means that is convenient to implement in computer-based calculations.

## 4.3. Modelling of Steady-State Pre-Fault Regimes

The pre-fault regime is mostly defined by the apparent powers of sources and loads, which themselves can be nonlinear functions of node voltages requiring the solution of a nonlinear equation system; an iterative solution can be used. This solution represents the sources and loads of the power system as current sources determined by the constant apparent power of the node and the L-L voltage:

$$J = I = \hat{S}/\left(\sqrt{3}\widehat{U}\right), \tag{4.4}$$

where $\hat{S}$ – the conjugated three-phase apparent power, VA;

$\widehat{U}$ – the conjugated L-L voltage, V.

This substitution can be justified because of the voltage regulation used in transmission networks and typically applied generator control strategies ($P_\mathrm{G}$, $Q_\mathrm{G}$ = const or $P_\mathrm{G}$, $|U|$ = const). Due to this substitution the branch EMF source vector $\boldsymbol{E}$ = 0 V and the equation system of the nodal potential method can be modified into

$$Y\boldsymbol{U} = \boldsymbol{I} + \boldsymbol{Y}_\mathrm{B}U_\mathrm{B} = \widehat{D}_\mathrm{S}\widehat{\boldsymbol{U}}^{-1} + \boldsymbol{Y}_\mathrm{B}U_\mathrm{B}, \tag{4.5}$$

where $\widehat{\boldsymbol{U}}^{-1}$ – a vector of inverse conjugated L-L nodal voltages ($\widehat{\boldsymbol{U}}_i^{-1} = 1/\widehat{\boldsymbol{U}}_i$), $\mathrm{V}^{-1}$;

$\widehat{D}_\mathrm{S}$ – a diagonal matrix of conjugated apparent powers connected to the power system nodes ($\widehat{D}_{\mathrm{S}ij} = \widehat{\boldsymbol{S}}_i/\sqrt{3}$ if $i = j$ and $\widehat{D}_{\mathrm{S}ij} = 0$ if $i \neq j$), VA.

The corresponding implementation of a numerical solution of equation system (4.5) is

$$\boldsymbol{U}_i^{k+1} = \sum_{j=1}^{i-1} C_{ij}\boldsymbol{U}_j^{k+1} + \sum_{m=i+1}^{n} C_{im}\boldsymbol{U}_m^{k} + \frac{1}{Y_{ii}}\left(\widehat{D}_{\mathrm{S}ii}\widehat{\boldsymbol{U}}_i^{-1\,k} + \boldsymbol{Y}_{\mathbf{B}i}U_\mathrm{B}\right). \tag{4.6}$$

In case of convergence issues of (4.6) a numerical implementation of inverse matrix method solution to (4.5) ($\boldsymbol{U} = Y^{-1}\widehat{D}_\mathrm{S}\widehat{\boldsymbol{U}}^{-1} + U_\mathrm{B}$) can be used instead:

$$\boldsymbol{U}_i^{k+1} = \sum_{j=1}^{i-1} Y_{ij}^{-1}\widehat{D}_{\mathrm{S}jj}\widehat{\boldsymbol{U}}_j^{-1\,k+1} + \sum_{m=i+1}^{n} Y_{im}^{-1}\widehat{D}_{\mathrm{S}mm}\widehat{\boldsymbol{U}}_m^{-1\,k} + U_\mathrm{B}. \tag{4.7}$$

When the node L-L voltages are estimated, the branch currents can be calculated by Eq. (4.3), taking into account that $\boldsymbol{E}$ = 0 V and using the L-E values of $\boldsymbol{U}$ and $U_\mathrm{B}$. Then the pre-fault EMF of the generators can be calculated, adding the voltage drop in the stator winding to the generator busbar L-E voltage.

## 4.4. Modelling of Transient Regimes Using a Numerical Inverse Laplace Transform

The base approach to the calculation of power system transients is to compose the differential equations that are based on Kirchhoff's laws for static linear circuits and include mechanical processes, and then solve the obtained equation system. Most often this will be done using numerical methods such as the trapezoidal rule, Euler's and Runge–Kutta methods [116], [117]. An approximate numerical inverse Laplace transform based on decomposition into a Fourier series was tested in this study, which obtains the time domain function using the values of the function in the Laplace domain $F(s)$ ($s = c + \mathrm{i}\omega$, $\mathrm{i} = \sqrt{-1}$) calculated for equally distributed values of the real part axis $\mathrm{Re}(s) = c$ [118], [119]. The following equation was derived to determine the coefficients for the sine series:

$$\sum_{i=0}^{m}\left(\left[\binom{2m}{i}-\binom{2m}{i-1}\right]S_{m-i}\right)=\frac{4^{m+1}}{\pi}\sigma F\big((2m+1)\sigma\big). \tag{4.8}$$

where $S_{m-i}$ – coefficients of the sine series;

$\sigma$ – a freely chosen positive real number;

$\binom{2m}{i}=\frac{(2m)!}{i!(2m-i)!}$ – $i$ combinations of $2m$; $m = 1, 2, \ldots, \infty$; $i = 0, 1, 2, \ldots, m$.

These sine series coefficients can be used to obtain the original time domain function:

$$f(t)=\sum_{i=0}^{m}\{S_i \sin[(2i+1)\arccos(\mathrm{e}^{-\sigma t})]\}. \tag{4.9}$$

Testing showed that the substitution of $F(s)$ with $F(s + a)$ used in this approach also often results in an incorrect time domain function if AC sources are present. Therefore, the presented method is useful mainly to calculate the transients of DC circuits or DC components of AC transients. However, this approach can be used with the topological nodal potential method but using state equations in the Laplace domain.

## 4.5. Modern Distance Protection Terminal Under Scrutiny – Testing Experience

There is a special but fairly common type of L-E faults in the Baltic region that should be highlighted – fallen-tree faults [1], [120], which demonstrate how significant the influence of the remote-end power system infeed can be. They sometimes have additional nonstationary resistance to earth during the burnout of the trunk of the tree, and oscillograms of DP apparent impedance showed that the burnout can be slow with a delayed fall of the apparent impedance [121]. In order to test the influence of such faults on DP performance, a modern digital OHTL protection and automation terminal [122] was tested using a virtual-real laboratory (simulations with MATLAB SimPowerSystems, signal generation with ISA DRTS 64 from a COMTRADE file). The results of the experimental testing showed that stationary fault path resistance could prevent operation of a backwards-directed reservation zone for L-L-E and L-E faults, and for L-E faults the presence of the transient resistance component caused additional time delays before the zone of operation was triggered (Figs. 4.1 and 4.2).

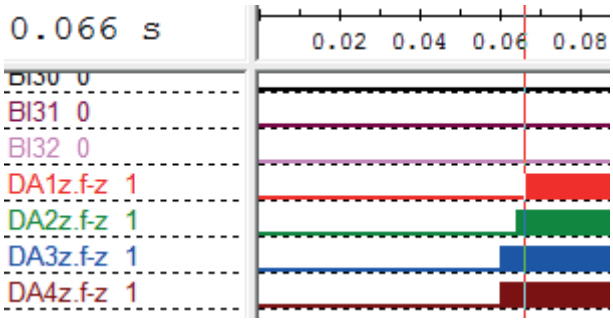


Fig. 4.1. Trigger times of DP L-E zones in case of a metallic fault [123].

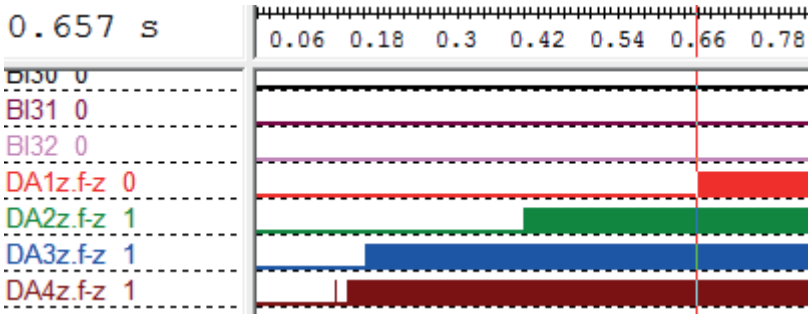


Fig. 4.2. Trigger times of DP L-E zones when the fault has a transient resistance [123].

This negative effect of fault earth path resistance for L-E faults can be avoided by using the proposed method because it estimates the value of equivalent fault path resistance and uses steady-state phasor values determined after signal processing.

## 4.6. Conclusions

1. Topological modelling of power systems with equivalent circuits combined with the nodal potential (admittance) method in the matrix form result in flexible and easy-to-implement computer-based fault and pre-fault regime modelling applications.
2. The presence of fault path resistance negatively affects the performance of the existing digital DP terminal both for L-E and L-L-E faults, especially in case of fallen-tree faults that can result in significant additional time delays.

# 5. APPLICATION OF THE ESTIMATION OF POWER SYSTEM MODEL PARAMETERS FOR FAULT LOCATION AND DISTANCE PROTECTION

## 5.1. The Framework of the Model Parameter Estimation Method

The proposed parameter estimation method is defined as an optimisation task, which minimises the difference between the measurements from the controlled substation and the corresponding outputs of a mathematical model. It is performed in two separate stages: an estimation of pre-fault regime and then the fault regime parameters, thus decreasing the number of unknown parameters for each individual stage. The first stage should be performed online at regular time intervals or after a significant change in any of the measured parameters: the busbar voltages, currents and power flows of the branches connected to the substation. The parameters estimated in the first stage are the real and imaginary powers of the main generation and load nodes and the PS resistance and reactance of links to the controlled branches if simplifications of the model are used. The estimated pre-fault model parameters are used to calculate the equivalent source EMFs for the fault model. The second stage of the estimation is initiated by a start logic, which determines the fault type and the moment of fault occurrence. The same measurements from the substation are recorded and used for estimation of the fault distance α, the equivalent fault path resistance $R_F$, and if necessary, NS and ZS equivalent resistance and reactance to the controlled branches. Both parameter estimation stages use the same optimisation and objective function (the difference between measurements and the output of a mathematical model):

$$f_{\mathrm{OBJ}} = \sum_{i=1}^{N_{\mathrm{MEA}}} K_{\mathrm{W}i} \left( \frac{y_i - y_{\mathrm{m}i}}{y_i} \right)^2, \tag{5.1}$$

where $K_{\mathrm{W}i}$ – the weight coefficient of the $i$-th parameter;

$N_{\mathrm{MEA}}$ – the number of measurements used for the estimation process;

$y_i$ and $y_{\mathrm{m}i}$ – the measured value of the $i$-th parameter and the corresponding model output.

The optimisation iteratively adjusts the values of the parameters being estimated, until the convergence criteria for the particular stage are met, ensuring that the objective function reaches a value close to the global minimum.

## 5.2. Modified Randomised Search Initially Tested for Estimation of Model Parameters

Considering that the objective function uses multiple parameters, which in most cases will be nonlinear functions of the estimated parameters (Fig. 6.1), it was suspected that the resulting function can have false extrema. Therefore, the first optimisation approach tested was a randomised search with a constriction procedure, which first randomly generated a vector of unknown parameter values $\boldsymbol{X}$ within the given search space limitations $\boldsymbol{X}_{\mathrm{min}}$, $\boldsymbol{X}_{\mathrm{max}}$.

These values are introduced into the model and its outputs and corresponding measurements are used to determine the objective function according to (5.1). This process is repeated until a certain number of improvements $N_{\mathrm{IMPR}}$ are reached, when the search space limitations are reduced:

$$\boldsymbol{X}_{\mathrm{max,min}} = \boldsymbol{X}_{\mathrm{B}} \pm \boldsymbol{X}_{\mathrm{N}}(\boldsymbol{K}_{\%}/(200s)), \tag{5.2}$$

where $\boldsymbol{X}_{\mathrm{min}}$ and $\boldsymbol{X}_{\mathrm{max}}$ – vectors of minimum and maximum possible $\boldsymbol{X}$ values;

$\boldsymbol{X}_{\mathrm{B}}$ –vector $\boldsymbol{X}$ with the currently smallest value of the objective function;

$\boldsymbol{K}_{\%}$ – the maximum difference from the nominal or average values of $\boldsymbol{X}$ elements, %;

$\boldsymbol{X}_{\mathrm{N}}$ – a vector of the nominal or average values of $\boldsymbol{X}$ elements;

$s$ – the step number of the parameter estimation process.

The described process is repeated until the rate of change of the objective function falls below a setting (here $\mathrm{d}f_{\mathrm{OBJ}} \leq 0.001$ was used).

The proposed method with this optimisation tool was tested for the DP and compared with the classical DP algorithm described in [11] and [124]. The testing showed that the powers of the two generators and two loads considered were estimated with errors within 2 % and that the proposed method would provide apparent impedances that ensure correct DP operation. On the other hand, the classical DP algorithm would operate with additional time delays even when a relatively small fault path resistance was present (see the black quadrangles in Fig. 5.1).

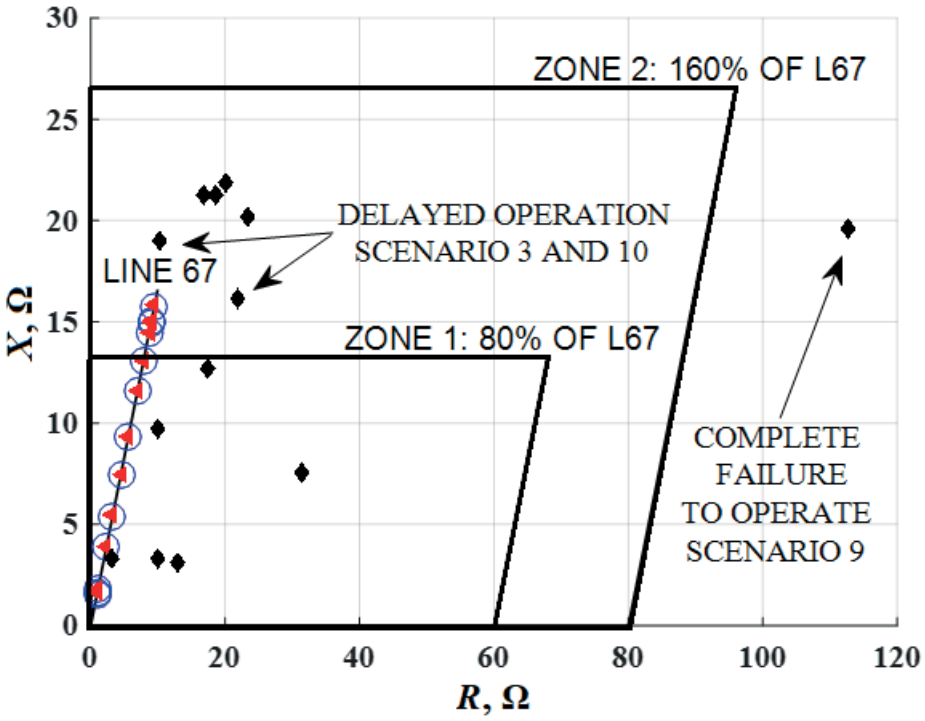


Fig. 5.1. Comparison of apparent impedances obtained by the classical DP algorithm and the proposed method in the *R*–*X* plane [125].

The testing of the proposed method with this optimisation tool for FL demonstrated not only a high accuracy, but also that in comparison with an existing one-terminal-measurement-

based FL [122] this accuracy was not affected by the pre-fault power flow (see Fig. 5.2 where the white surface represents the existing FL and the coloured surface corresponds to the proposed method) [126].

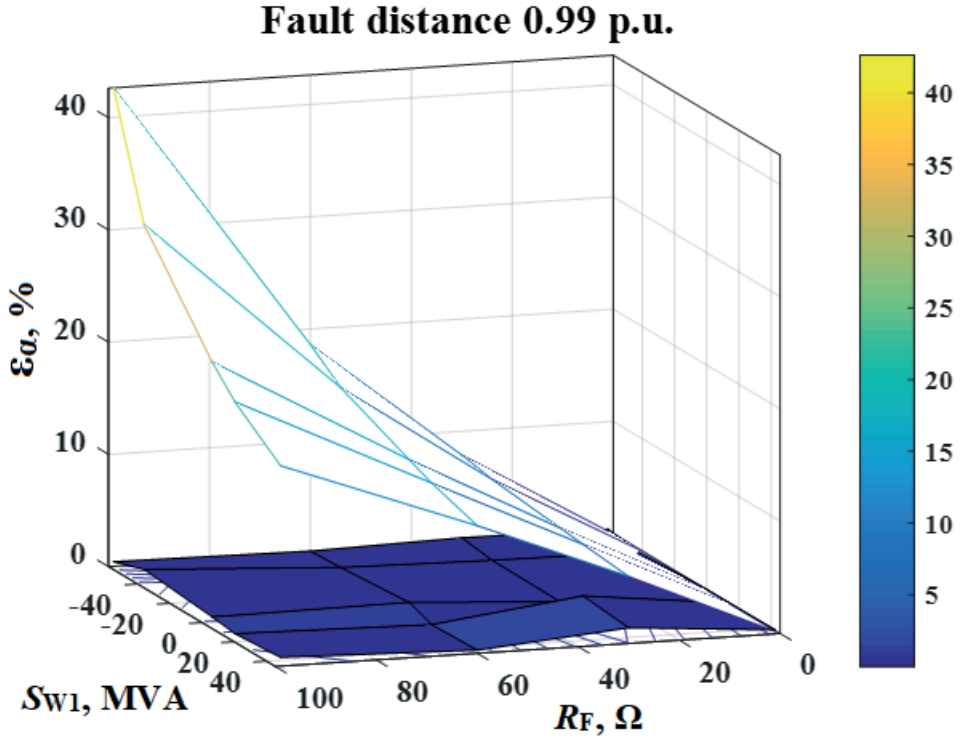


Fig. 5.2. Fault distance estimation errors $\varepsilon_\alpha$ in different cases of pre-fault power flows $S_{W1}$, fault path resistances $R_F$ and a fixed fault distance of 99 % [126].

While these results indicate a high accuracy compared with the existing one-terminal-measurement-based DP and FL algorithms, the application of modified randomised search did require significant calculation time, which prompted the search for a different optimisation tool.

## 5.3. Modified Genetic Algorithm Applied for Estimation of Model Parameters

GA is a versatile optimisation tool that has been useful in similar tasks [50], [127], [128], which is relatively easy to implement and which with safety mechanisms can avoid convergence to local extrema if any are present in the objective function [129], [130]. It utilises natural selection based on the fitness (objective function) of different solution scenarios, obtaining the best solution with several typically used steps or operators: pairing of parent individuals, recombination (reproduction), mutation of offspring individuals, determination of the adaptability of parent and offspring individuals, selection of the next generation [23], [128]–[130]. This optimisation represents each individual or solution by a chromosome, which is a consequent chain of values of unknown parameters in binary.

The GA version used in this Thesis starts with randomly generating a large group (here 3000) of solution variants to reduce the influence of first-generation mean fitness compared to the composition of the objective function. Then the fitness of these solutions is calculated

using (5.1) and a separate selection is performed to create the first generation for the main GA cycle. Before the main GA cycle, the generation number $N_{GEN}$ is set to 1 and the number of stagnating generations $N_{STAG}$ is set to 0. The main GA cycle begins with the pairing of the parent individuals according to the "outbreeding" approach and determination of the probability of the occurrence of any mutation of the chromosome of offspring individuals $P_{MUT}$ using the "incest" approach. Then follows the recombination or creation of a group of offspring individuals sized *POPsize* (here, equal to 20) from the chromosomes of parent individuals applying an approach similar to "triadic crossover". The third step is the mutation according to the approach of "density mutation" with $P_{MUT}$ and the probability of the mutation of a particular gene $P_{GENEMUT}$. The next step is the selection that chooses the next generation from parent and offspring or randomly generated individuals using the "elite selection" for 10 % of next-generation members and the "roulette-wheel selection" approach for the remaining members [129], [130]. When the selection process is finished, the difference between the maximum and minimum fitness values $\Delta f_{OBJ}$ and the maximum Hamming distance max $d_{HAMM}$ of the next generation is determined for convergence criteria tests. Next, the differences of the maximum and minimum values of the population objective functions $\Delta$max $f_{OBJ}$ and $\Delta$min $f_{OBJ}$ between generations are calculated and compared with a stagnation margin (here, 0.1 %), and if both are below this limit, $N_{STAG}$ is increased by 1; otherwise, $N_{STAG}$ is reset to 0. When $N_{STAG}$ exceeds the number of permissible stagnations (here, 20), additional 1000 individuals are randomly generated with reduced limitations and the selection process is repeated. Finally, the convergence criteria are tested: $N_{GEN}$ exceeds min $N_{GEN}$ = 50, $\Delta f_{OBJ}$ is below min $\Delta f_{OBJ}$ = 0.05 p.u. and max $d_{HAMM}$ is below min $d_{HAMM}$ = 0.05 p.u. The case study results obtained with the proposed method using the GA will be presented separately in Chapter 7 of the Thesis.

## 5.4. Conclusions

1. The division of the model parameter estimation into two stages reduces the amount of unknown data that have to be determined after fault inception, thus making the second stage more feasible.
2. Since the objective function for the estimation of unknown parameters can have false extrema, an optimisation tool that can find the global extremum in such conditions is necessary.
3. The accuracy of the existing digital FL using one-terminal measurements has a high degree of dependence on the pre-fault power flow, especially if it is oriented towards the substation, which is not present for the proposed applications of parameter estimation for DP and FL.
4. The proposed method provided a sufficient accuracy for both estimation stages, when tested with the modified randomised search, which outperforms existing one-terminal-measurement-based DP and FL algorithms.
5. The initially tested modification of a randomised search provided satisfactory results, but it did require significant computation time, which led to the adoption of the GA.

# 6. SYNTHESIS OF OPTIMAL OBJECTIVE FUNCTION FOR ESTIMATION OF MODEL PARAMETERS

The framework of the proposed method that is described in Chapter 5 is universal in nature, but the question of the synthesis of an optimal version of the objective function (5.1) remains. This can be achieved by using weight coefficient $K_{Wi}$ and/or selecting optimal parameter group $Y$. In case of the pre-fault regime, the parameter group will have a limited size as the pre-fault regime in a transmission system should be practically symmetrical [131], [132]. The faults, on the other hand, can be expected to be mainly asymmetrical [54], [133], [134] and the parameter group could include real and imaginary parts or magnitudes, angles of phase quantities, symmetrical components of busbar voltages and branch currents and apparent power for each substation branch. This could result in an exceedingly large and hard-to-manage parameter group. Thus, the focus will be on the synthesis of the optimal objective function for the second estimation stage. The initial attempt to optimise the weights $K_{Wi}$ with an additional outer GA cycle was slow and did not yield an unambiguous result, and a fixed value for $K_{Wi}$ of 100 was assumed, testing different parameter selection strategies and sizes of parameter groups instead.

## 6.1. Fault Parameter Selection Strategies

Considering that the objective function is defined as the difference between measured and modelled parameter values, one can expect that the sensitivity of the parameter to changes in the fault distance α is vital, otherwise the optimisation can randomly select any α. However, after examining the graphs of different parameters, it can be seen that even parameters that are highly dependent on $\alpha$ in most cases also retain significant dependence on the fault path resistance $R_F$ (Fig. 6.1).

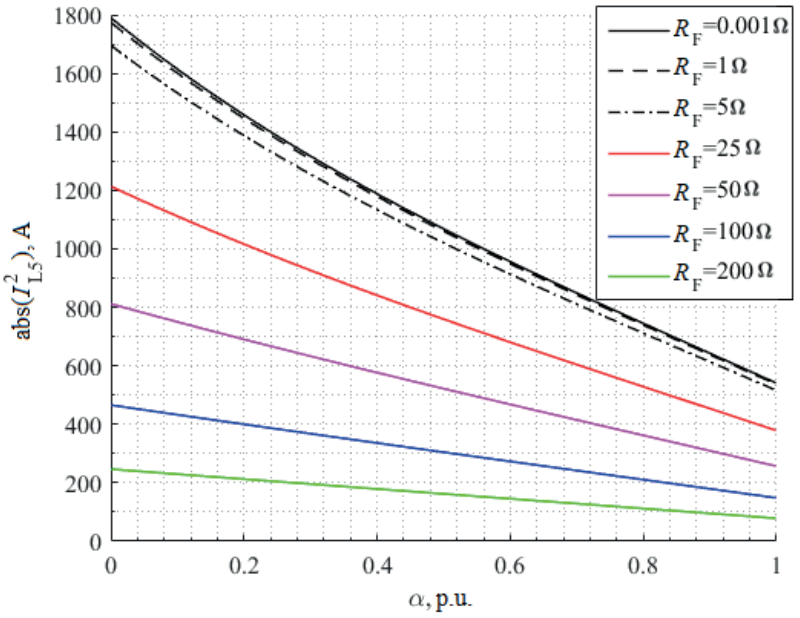


Fig. 6.1. The absolute value of the NS current of the faulted line.

Based on the previous considerations, two parameter selection strategies were proposed: a conservative strategy and an opportunistic one. The idea behind the opportunistic strategy is to sort all the available measured or derived parameters only according to their maximum sensitivity to changes in α values $\max \Delta y_i$. The conservative strategy first tests if the minimum sensitivity of an available parameter $\min \Delta y_i$ reaches a certain minimum limit (here 0.01 %) and the change of the parameter is monotonic to make the global minimum of the objective function more unambiguous.

To evaluate the sensitivity of the measured parameters, numerical calculations of fault regimes with different α for several $R_F$ values were performed, and then discrete differences $\Delta y_i/\Delta\alpha \approx \mathrm{d}y_i/\mathrm{d}\alpha$ were calculated. Additionally, fixed fault distance intervals were used to focus on the differences of the analysed parameter, $\Delta y_i$. In order to adequately compare the available parameters, adaptive base quantities were chosen. The maximum value of the faulted phase current and the apparent power magnitude of the particular branch (obtained from simulations of all the analysed α and $R_F$ values) was used for the corresponding phase current, apparent power, and their symmetrical components. Similarly, for voltage parameters, the maximum magnitude of the faulted phase value was used. The base quantity for the fault distance obtained by the existing FL algorithm was the line length. Simulations used for parameter analysis considered fault distances with a step of 5 % of OHTL and $R_F$ values of 0.001 Ω, 1 Ω, 5 Ω, 25 Ω, 50 Ω, 100 Ω, 200 Ω. The parameters considered for the selection process were:

- the magnitudes, real and imaginary parts of faulted phase voltage from substation busbars and its PS, NS, ZS quantities;
- the magnitudes, real and imaginary parts of faulted phase current and apparent power from all the branches connected to the substation and their PS, NS, ZS quantities;
- the fault distance calculated by an existing FL algorithm [122].

## 6.2. Development of Future Strategies of Parameter-Selection-Based Analysis of Objective Function

The analysis of surfaces of the objective function in Section 7.2 of the Thesis shows that these may have distortions and false extrema that can be around the true fault distance α*, the true fault path resistance $R_F$* value or in other configurations. The last two could cause significant fault distance estimation errors, which prompted further analysis on the surfaces of the objective function created by individual parameters and their interactions. According to (5.1), for a single parameter $y$ any point in the search space (values of at least α and $R_F$), which has parameter value $y = y^* = y(\alpha^*, R_F^*)$, will yield $f_{OBJ} = 0$. Thus, when using only one parameter, the optimisation can determine α accurately with certainty only if the parameter is invariant of $R_F$ and function $y(\alpha)$ is monotonic. Otherwise, the surface will have value 0 at all points where the surface $y = y(\alpha, R_F)$ crosses a horizontal plane defined by the measured value $y(\alpha^*, R_F^*)$. The orientation of the lines created by points $f_{OBJ} = 0$ (minimum ravines) can be partially assessed with 2D graphs such as Fig. 6.1. A significant number of parameters analysed were monotonic and the characteristics for different $R_F$ values were in consequent

order, but even for these parameters there was different orientation of minimum ravines. Some were limited by certain fault distance intervals (Fig. 6.2).

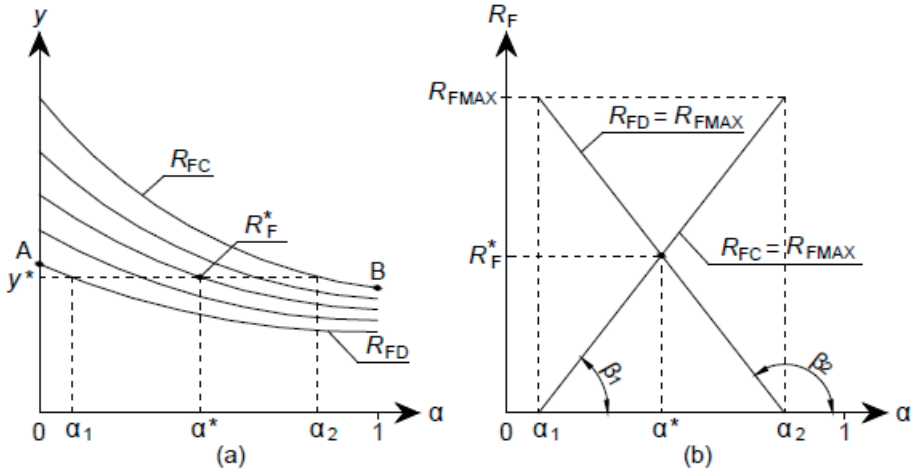


Fig. 6.2. A monotonic graph of the values of parameter *y* (a), and orientation of minimum ravines limited by a fault distance interval (b).

This is true if the maximum point of the characteristic, which has the lowest absolute values *y*(A), is above the minimum point of the characteristic, which has the highest absolute values *y*(B) (Fig. 6.2 (a)). If *y*(A) < *y*(B), any point (α, $R_F$) with a parameter value *y*(A) < *y* < *y*(B) will have a minimum ravine with limited $R_F$ values (Fig. 6.3).

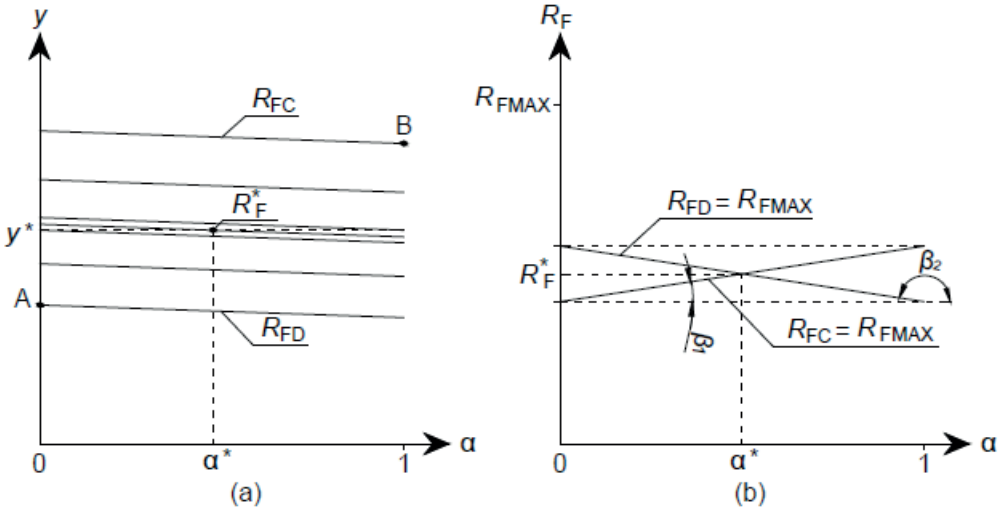


Fig. 6.3. A monotonic graph of the values of parameter *y* (a), and orientation of minimum ravines limited by a fault path resistance interval (b).

There are also parameters with mixed order of characteristics and ones that result in multiple minimum ravines simultaneously (function *y*(α) is ambiguous). After further analysis of different minimum ravines and objective functions created by their interaction, a grouping approach for the future parameter selection strategy was devised. One of the groups would have parameters with either a distinctly acute or a distinctly obtuse angle β (sensitivity to $R_F$), and the second group should have angle β as close to 90° as possible (sensitivity to α). The parameter ranking within those groups would be determined by how close their angle β can be

to the group limiting angle values, and the resulting parameter group $Y$ used by the optimisation would be assembled from both subgroups according to subgroup ranking.

## 6.3. Conclusions

1. One approach to the selection of measured parameters for use in the objective function is to sort them only by their sensitivity to changes in the fault distance, but it often results in objective functions with surface distortions and false extrema, which increases the risk of inaccurate fault distance estimation.
2. Analysis of measurable or derived parameter curves for different fault distance and resistance values could be used to obtain parameter groups that would result in fewer distortions in the surface of the objective function and a more distinct global extremum.

# 7. TESTING OF THE PROPOSED PARAMETER ESTIMATION METHOD AND PARAMETER SELECTION STRATEGIES

## 7.1. The Power System Used for the Case Studies

The power system used for studying the characteristics of the available parameters and the testing of implementation of the proposed method for FL using GA is presented in Fig. 7.1.

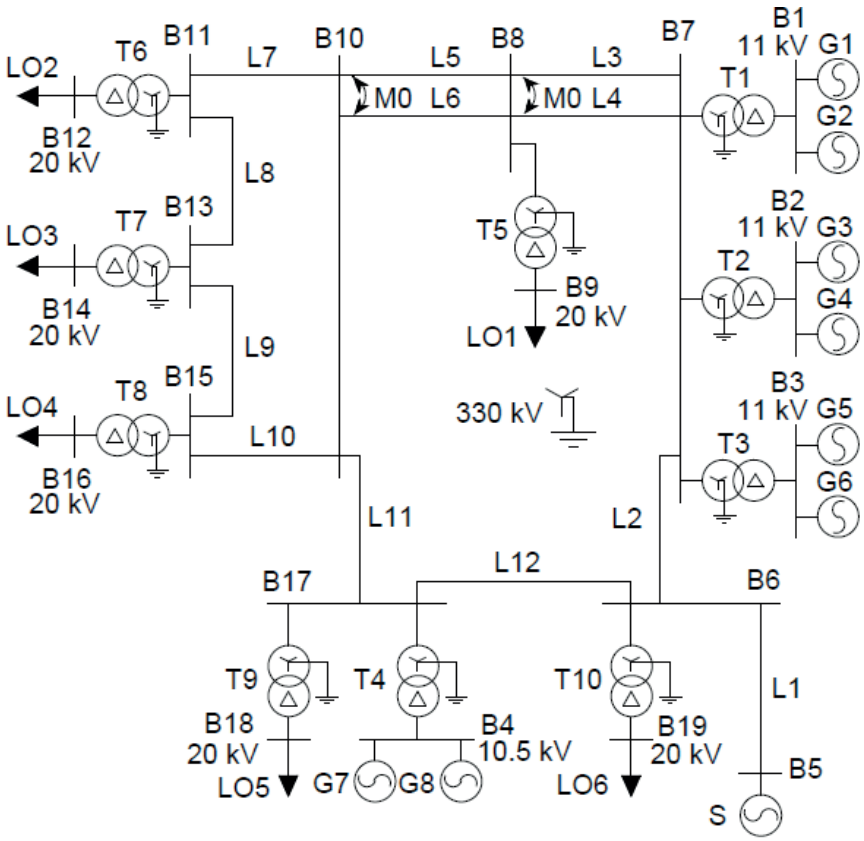


Fig. 7.1. The case study power system.

The potential power limits of randomly generated pre-fault regimes were 0–120 % of the nominal value for the active and reactive power of the loads as well as the active power of generators, but limits −120–120 % were used for the reactive power of generators. The testing results presented below will consider the substation depicted with a controlled bus B10 (denoted as RELAY 1) with scenarios of L-E faults in lines L5, L6 and L11 (denoted as FAULT 1, FAULT 2 and FAULT 6). The data of the case study power system elements and full testing results are provided in the full text of the Thesis.

## 7.2. Results of Parameter Selection

After reviewing the results of the parameter analysis, groups of up to 20 parameters were chosen, ranked within those groups according to Section 6.1. The obtained parameter groups

for RELAY1 are presented in Table 7.1 (here, "REDI" denotes the existing one-terminal-measurement-based FL algorithm [122]).

Table 7.1

The Parameter Groups According to the Proposed Parameter Selection Strategies

| RANK | FAULT1 | | FAULT2 | | FAULT6 | |
|---|---|---|---|---|---|---|
| | Conservative | Opportunistic | Conservative | Opportunistic | Conservative | Opportunistic |
| 1. | Re ($I_{L6}$) | REDI | Re ($I_{L5}$) | REDI | $\lvert I^0_{L7}\rvert$ | REDI |
| 2. | Im ($S^1_{L6}$) | Im ($I_{L6}$) | Im ($S^1_{L5}$) | $\lvert I_{L5}\rvert$ | $\lvert I^0_{L10}\rvert$ | $\lvert I_{L10}\rvert$ |
| 3. | $\lvert I^0_{L7}\rvert$ | $\lvert I_{L6}\rvert$ | $\lvert I^0_{L7}\rvert$ | Im ($I_{L5}$) | $\lvert I_{L5}\rvert$ | $\lvert I_{L7}\rvert$ |
| 4. | $\lvert I^0_{L10}\rvert$ | Re ($I_{L6}$) | $\lvert I^0_{L10}\rvert$ | Re ($I_{L5}$) | $\lvert I_{L6}\rvert$ | Im ($I_{L7}$) |
| 5. | Im ($S^2_{L6}$) | $\lvert I_{L5}\rvert$ | Im ($S^2_{L5}$) | $\lvert I_{L6}\rvert$ | Re ($I_{L11}$) | $\lvert I^0_{L7}\rvert$ |
| 6. | Re ($S^1_{L6}$) | Im ($I_{L5}$) | Re ($S^1_{L5}$) | Im ($I_{L6}$) | $\lvert I^0_{L11}\rvert$ | $\lvert I^0_{L10}\rvert$ |
| 7. | Re ($I_{L5}$) | $\lvert I^1_{L6}\rvert$ | Re ($I_{L6}$) | $\lvert I^1_{L5}\rvert$ | Re ($I_{L5}$) | Im ($I_{L10}$) |
| 8. | $\lvert I_{L11}\rvert$ | $\lvert I^2_{L6}\rvert$ | $\lvert I_{L11}\rvert$ | Im ($S^1_{L5}$) | Re ($I_{L6}$) | Im ($I^0_{L7}$) |
| 9. | Re ($I^1_{L6}$) | $\lvert I_{L10}\rvert$ | Re ($I^1_{L5}$) | $\lvert I^2_{L5}\rvert$ | $\lvert I^2_{L5}\rvert$ | Im ($I^0_{L10}$) |
| 10. | Re ($I^2_{L6}$) | Im ($I^1_{L6}$) | Re ($I^2_{L5}$) | Im ($I^1_{L5}$) | $\lvert I^2_{L6}\rvert$ | $\lvert I_{L11}\rvert$ |
| 11. | $\lvert I^0_{L5}\rvert$ | Im ($I^2_{L6}$) | $\lvert I^0_{L6}\rvert$ | $\lvert I_{L7}\rvert$ | $\lvert I^1_{L5}\rvert$ | Im ($I_{L11}$) |
| 12. | Re ($I^0_{L10}$) | Im ($S^1_{L6}$) | Im ($S^2_{L6}$) | Im ($I^2_{L5}$) | $\lvert I^1_{L6}\rvert$ | $\lvert I_{L5}\rvert$ |
| 13. | Im ($S^2_{L5}$) | $\lvert I_{L7}\rvert$ | Re ($I^0_{L7}$) | $\lvert I_{L10}\rvert$ | $\lvert I^2_{L11}\rvert$ | $\lvert I_{L6}\rvert$ |
| 14. | Re ($I^0_{L6}$) | Im ($I_{L10}$) | $\lvert I^2_{L6}\rvert$ | Im ($I_{L7}$) | $\lvert I^0_{L5}\rvert$ | Im ($I_{L5}$) |
| 15. | $\lvert I^2_{L5}\rvert$ | $\lvert I^0_{L7}\rvert$ | Re ($I^0_{L5}$) | $\lvert I^0_{L7}\rvert$ | $\lvert I^0_{L6}\rvert$ | Im ($I_{L6}$) |
| 16. | Re ($S^1_{L5}$) | $\lvert I^0_{L10}\rvert$ | Re ($S^1_{L6}$) | $\lvert I^0_{L10}\rvert$ | $\lvert U^2_{B10}\rvert$ | Re ($I_{L7}$) |
| 17. | Re ($I_{L11}$) | Im ($I^0_{L7}$) | Re ($I_{L11}$) | Im ($I_{L10}$) | $\lvert U^0_{B10}\rvert$ | Re ($U_{B10}$) |
| 18. | Re ($I^0_{L5}$) | Im ($I_{L7}$) | Re ($I^0_{L6}$) | Im ($I^0_{L7}$) | Re ($I^1_{L5}$) | $\lvert U_{B10}\rvert$ |
| 19. | Re ($I^2_{L5}$) | Im ($I^0_{L10}$) | Re ($I^2_{L6}$) | Im ($I^0_{L10}$) | Re ($I^1_{L6}$) | Re ($I_{L10}$) |
| 20. | Re ($I^1_{L5}$) | Im ($S^2_{L6}$) | Re ($I^1_{L6}$) | Im ($S^2_{L5}$) | Re ($I^2_{L5}$) | Re ($I^0_{L10}$) |

Table 7.1 also shows that the selected parameter groups partially overlap. This happened because the ranking of the parameters according to the conservative strategy is also performed by the maximum sensitivity, but only after the testing of the additional criteria. Before discussing the testing of the obtained parameter groups, it should be briefly noted that a separate analysis of the surfaces of the objective function created using the proposed parameter selection strategies showed form distortions in some of the tested fault scenarios for both strategies. This confirmed that an optimisation capable of avoiding false extrema is necessary. Additionally, reduction of the number of available parameters performed during this analysis showed that smaller numbers of available parameters more often yield surfaces with additional false extrema and other form defects. Therefore, it can be suspected that the more parameters are used the more they damp distortions introduced by other parameters.

## 7.3. Testing Results for the Proposed Method

The proposed method with the GA as the optimisation tool and the described parameter selection strategies were extensively tested considering 20, 15, 10 and 5 parameters used in the objective function (5.1) and 1000 tests randomised pre-fault and fault scenarios for each of

these subcases. The focus of the testing was on the estimation of the fault parameters and the randomised pre-fault regime was assumed to be known. The maximum and mean values of estimation errors ε for α and $R_F$, the mean number of generations necessary for convergence $N_{GEN}$, and the upper boundary for α estimation errors covering 95 % of the expected values $\varepsilon_{\alpha B}$ for the tested cases are given in Table 7.2.

Table 7.2

The Results of Testing for RELAY1

| | STRATEGY | $N_{PAR}$ | max $\varepsilon_\alpha$, % | mean $\varepsilon_\alpha$, % | $\varepsilon_{\alpha B}$, % | max $\varepsilon_{RF}$, % | mean $\varepsilon_{RF}$, % | mean $N_{GEN}$ |
|---|---|---|---|---|---|---|---|---|
| FAULT1 | Opportunistic | 20 | 0.787 | 0.037 | 0.093 | 1.722 | 0.041 | 1125.9 |
| | | 15 | 1.457 | 0.039 | 0.102 | 1.540 | 0.038 | 1183.1 |
| | | 10 | 0.303 | 0.035 | 0.094 | 2.184 | 0.044 | 1252.9 |
| | | 5 | 0.768 | 0.035 | 0.079 | 2.168 | 0.064 | 1285.5 |
| | Conservative | 20 | 0.881 | 0.036 | 0.084 | 4.024 | 0.058 | 930.4 |
| | | 15 | 1.031 | 0.034 | 0.091 | 40.901 | 0.133 | 1280.2 |
| | | 10 | 0.772 | 0.039 | 0.114 | 4.888 | 0.097 | 989.8 |
| | | 5 | 0.848 | 0.041 | 0.130 | 25.885 | 0.142 | 1098 |
| FAULT2 | Opportunistic | 20 | 1.719 | 0.036 | 0.086 | 1.133 | 0.032 | 1161.1 |
| | | 15 | 1.735 | 0.038 | 0.090 | 4.290 | 0.041 | 1072.9 |
| | | 10 | 0.849 | 0.036 | 0.096 | 1.349 | 0.042 | 1013.5 |
| | | 5 | 2.029 | 0.036 | 0.090 | 1.758 | 0.067 | 974.5 |
| | Conservative | 20 | 0.893 | 0.033 | 0.078 | 49.60 | 0.149 | 1078.3 |
| | | 15 | 2.220 | 0.039 | 0.092 | 46.178 | 0.133 | 1049.6 |
| | | 10 | 3.379 | 0.043 | 0.101 | 6.518 | 0.093 | 1222.3 |
| | | 5 | 1.371 | 0.041 | 0.100 | 33.293 | 0.129 | 1446.2 |
| FAULT6 | Opportunistic | 20 | 2.685 | 0.085 | 0.363 | 0.455 | 0.030 | 2764.7 |
| | | 15 | 3.641 | 0.075 | 0.231 | 0.764 | 0.028 | 2114.1 |
| | | 10 | 3.595 | 0.078 | 0.262 | 1.218 | 0.035 | 3011.8 |
| | | 5 | 5.118 | 0.076 | 0.235 | 1.372 | 0.049 | 2863.1 |
| | Conservative | 20 | 2.613 | 0.082 | 0.309 | 0.721 | 0.031 | 2838.7 |
| | | 15 | 3.135 | 0.094 | 0.329 | 0.909 | 0.035 | 2436.1 |
| | | 10 | 4.024 | 0.123 | 0.447 | 1.204 | 0.045 | 4382.9 |
| | | 5 | 6.134 | 0.120 | 0.424 | 1.517 | 0.044 | 4934.2 |

The analysis of the testing results from Table 7.2 and other scenarios presented in the full text showed that the accuracy of α estimates for the proposed method seems to be lower for faults in single-circuit lines than for faults in double-circuit lines (Figs. 7.2 and 7.3) and for faults towards generators compared with faults towards load centres. This was the same for the mean number of necessary generations, but the accuracy of $R_F$ estimates was not affected. In cases of faults in single-circuit lines, the opportunistic strategy had a higher accuracy of α estimates, but for faults in double-circuit lines the conservative strategy performed equally or better. In terms of $R_F$, estimates the opportunistic strategy was more accurate, but in most cases the mean number of necessary generations was similar for both strategies. FAULT6 was especially challenging for the proposed method, having a case of α estimation error above 5 %, but this mainly indicates that the minimal parameter group size should be between 5 and

10. The upper boundary for 95 % of α estimation errors showed that in most cases this error will not exceed 0.12 % and for single-circuit line faults 0.45 % in contrast to the randomised search method that had errors mostly between 0.1–1.5 %.

In order to compare the performance of the proposed method with existing FL methods, FL algorithms using one-terminal measurements and two-terminal measurements of NS voltages and currents [122] were tested in the same randomised conditions. The results of this testing are presented in Table 7.3.

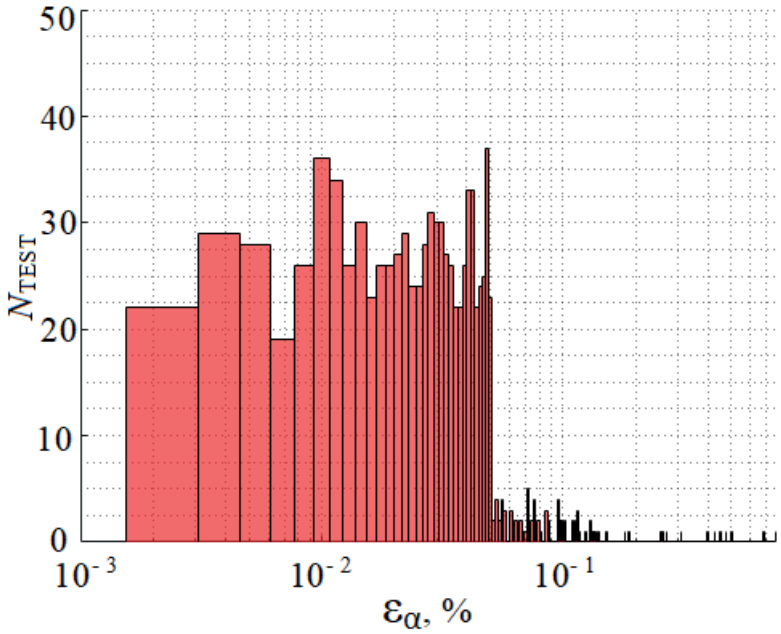


Fig. 7.2. The histogram of fault distance estimation error modulus obtained with opportunistic strategy FAULT1 and parameter count 5.

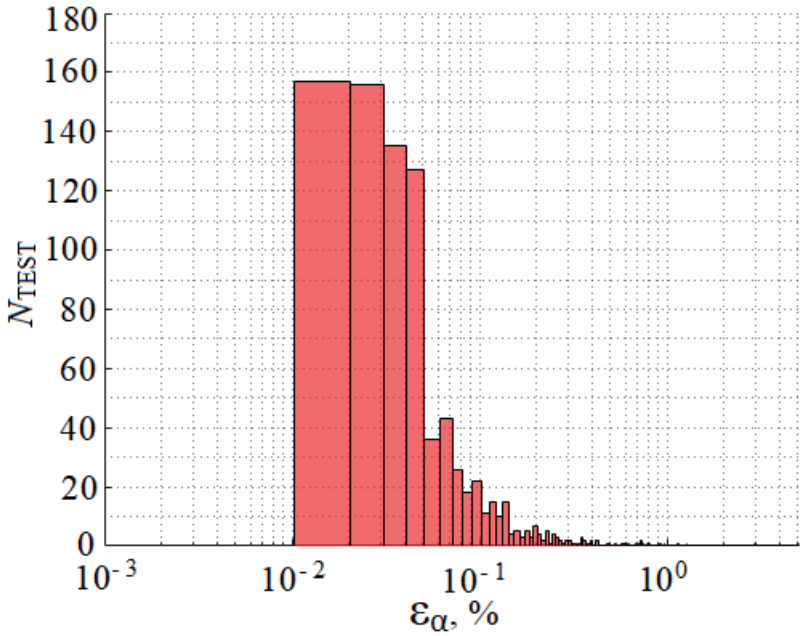


Fig. 7.3. The histogram of fault distance estimation error modulus obtained with opportunistic strategy FAULT6 and parameter count 5.

Table 7.3

The Results of Testing of Existing Fault Locators

| | Fault case | max $\varepsilon_\alpha$, % | mean $\varepsilon_\alpha$, % | $\varepsilon_{\alpha B}$, % |
|---|---|---|---|---|
| One-terminal-measurement-based fault locator | FAULT1 | 169.977 | 16.679 | 59.939 |
| | FAULT2 | 157.670 | 17.754 | 63.871 |
| | FAULT6 | 939.143 | 47.575 | 208.96 |
| Two-terminal-measurement-based fault locator | FAULT1 | 0.216 | 0.105 | 0.198 |
| | FAULT2 | 0.214 | 0.107 | 0.199 |
| | FAULT6 | 0.219 | 0.107 | 0.200 |

The comparison between the performance of the proposed method and the existing one- and two-terminal-measurement-based FL according to Tables 7.2 and 7.3 and full testing results showed that the accuracy of the FL using one-terminal measurements approached the accuracy of the proposed method only in few cases when considering the maximum error of α estimates. The two-terminal-measurement-based FL outperforms the proposed method in terms of maximum error of α estimates, but the mean errors and the upper boundaries for 95 % of error values were lower for the proposed method when faults occurred in double-circuit lines. Thus, the proposed method will often have a higher concentration of more accurate results across a large number of cases.

## 7.4. Conclusions

1. The updated version of the parameter estimation method using the GA clearly outperformed an existing one-terminal-measurement-based FL algorithm.
2. The updated version of the proposed method had higher maximum error values than the existing two-terminal-measurement-based FL method using NS quantities, but in terms of mean error and expected concentration of 95 % of fault distance estimation error values, the proposed method often outperformed the two-terminal-measurement-based method.

# 8. APPLICATION OF THE MODEL PARAMETER ESTIMATION AND TOPOLOGICAL MODELLING APPROACH FOR THE DEVELOPMENT OF AN ADAPTIVE SINGLE-POLE AUTOMATIC RECLOSING

The proposed application for ASPAR uses the topological modelling method both in symmetrical components to model the overall influence of the power system on the one-open-phase regime of the OHTL present during the dead time and in phase coordinates to more accurately model interactions between the healthy phases and the disconnected faulted phase. The fault distance estimated by the FL proposed in this Thesis is used to calculate the adaptive setting of the developed ASPAR method.

## 8.1. Modelling of High-Voltage Transmission Line in Phase Coordinates

In order to evaluate the possible parameters used for the ASPAR, a detailed OHTL model in phase coordinates was developed that considered the conductor self-impedance $Z_{\mathrm{W}}$, the ground (earth) wire impedance $Z_{\mathrm{GW}}$, all of the mutual coupling impedances $Z_{\mathrm{MAB}}$, $Z_{\mathrm{MBC}}$, $Z_{\mathrm{MCA}}$, $Z_{\mathrm{MAGW}}$, $Z_{\mathrm{MBGW}}$, $Z_{\mathrm{MCGW}}$, capacitances between phases $C_{\mathrm{AB}}$, $C_{\mathrm{BC}}$, $C_{\mathrm{CA}}$, between the phases and the earth $C_{\mathrm{AG}}$, $C_{\mathrm{BG}}$, $C_{\mathrm{CG}}$ as well as between the phases and the earth wire $C_{\mathrm{AGW}}$, $C_{\mathrm{BGW}}$, $C_{\mathrm{CGW}}$. The calculation methods for determination of the aforementioned line parameters according to [135]–[137] were also provided. This model included EMF sources at both ends of the line, which are busbar L-E voltages obtained by solving the problem of two simultaneous open-phase faults with the whole network model according to the description in Section 3.3.

## 8.2. Dynamic Arc Model Used for Development and Testing of the Adaptive Automatic Reclosing Method

The secondary arc model used during the dead time is an implementation of the piecewise linear volt-ampere cyclogram (dependence of the voltage gradient on the secondary arc current) combined with time-dependent arc reignition. The secondary arc reignition voltage is calculated and applied during the arc extinctions [135]:

$$U_{\mathrm{re}} = (5 + 50T_{\mathrm{e}})(t - T_{\mathrm{e}})h(t - T_{\mathrm{e}}), \tag{8.1}$$

where $U_{\mathrm{re}}$ – the secondary arc reignition voltage, kV/cm;

$T_{\mathrm{e}}$ – the time from the beginning of the secondary arc till the fault arc extintion (intermediate of final), s;

$t$ – the simulation time, s;

$h(t - T_{\mathrm{e}})$ – a delayed step function (0, $t < T_{\mathrm{e}}$; 1, $t > T_{\mathrm{e}}$).

One of the main reasons why the secondary arc becomes extinguished is the elongation of the arc channel, which in the Thesis is considered according to [138], with the initial arc length being by 10 % larger than the phase insulator length.

The primary arc (before fault disconnection) model is similar to the secondary arc but the length of the arc channel is assumed to be constant. The primary arc cyclogram used in this Thesis is a piecewise linearisation of the volt-ampere cyclogram shown in [139]. Both of the described arc models were implemented in a MATLAB SimPowerSystems model, where two Thevenin's equivalents of power systems S1 and S2 are connected by two line π-sections representing the parts of the line before and after the fault. The restrike that occurs if the AR command is given prematurely or the fault is permanent in nature is performed by switching from the model of the secondary arc to the primary arc one. The instantaneous current and voltage of the fault arc during successful SPAR is shown in Fig. 8.1 (the primary arc model is connected 50–100 ms and the secondary arc model – 100 ms after the start of the simulations) displaying higher harmonic distortions of the arc current, increasing of the arc reignition voltage, and the increase of the fault point voltage with a DC offset after arc extinction at approximately 0.369 s.

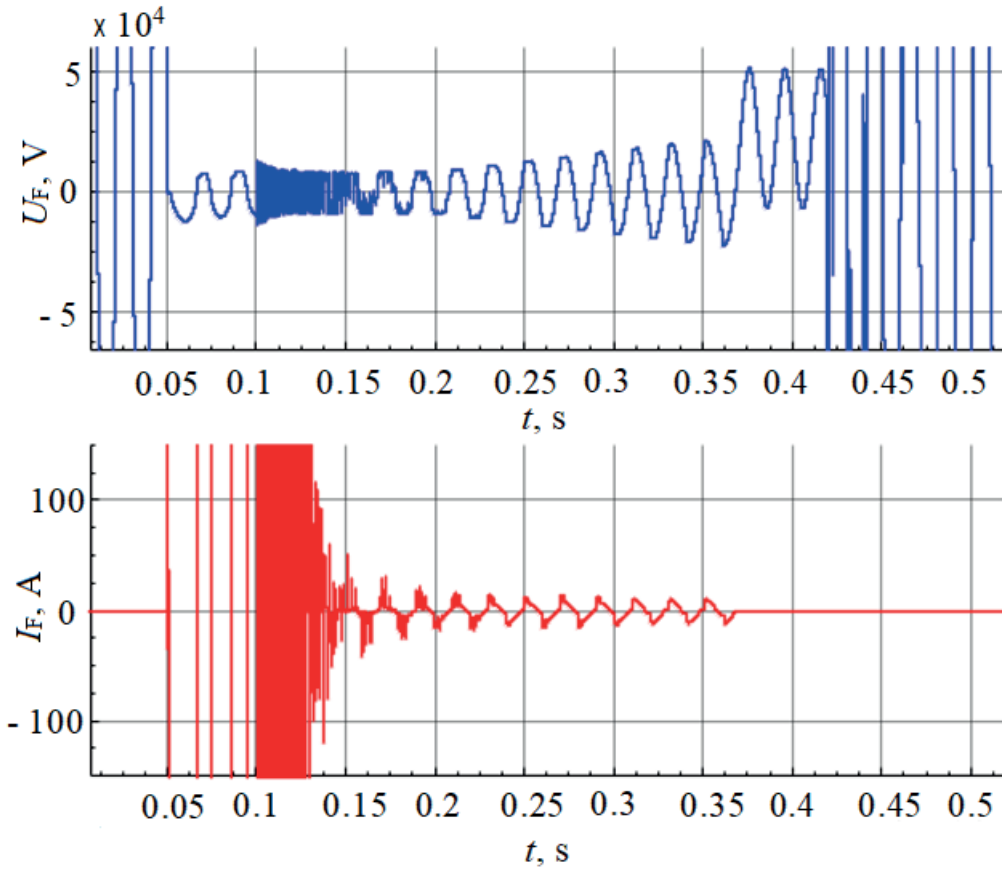


Fig. 8.1. The arc voltage and current at the fault point during a successful SPAR [135].

## 8.3. The Proposed Adaptive Single-Pole Automatic Reclosing Method

Analysis of the faulted phase line-side voltage $U_F$ and its real and imaginary parts obtained from both steady-state and dynamic simulations after filtering and discrete derivatives of these parameters allowed forming criteria for ASPAR to determine the moment of arc extinction and the time to issue a reclose command. The following criteria were defined: the absolute value of the real part of the faulted phase line-side voltage exceeds a

setting $|\mathrm{Re}\,(U_\mathrm{F})| \geq S_{\mathrm{Re}2}$, the absolute values of the discrete derivatives of the real and imaginary part of the same voltage fall below different settings $|\Delta\mathrm{Re}\,(U_\mathrm{F})/\Delta t| \leq S_{\mathrm{Re}}$, $|\Delta\mathrm{Im}\,(U_\mathrm{F})/\Delta t| \leq S_{\mathrm{Im}}$ and the RMS value of the same voltage is below a setting $|U_\mathrm{F}| \leq S_{\mathrm{ABS}}$. These criteria are supplemented with a start signal, which indicates the open state of the CBs, an additional time delay $\Delta t_1$, which first includes 5–10 ms of switch on delay to prevent undesirable SPAR operation during intermediate arc extinctions and 20 ms of delay before the final reclose command is issued to provide time for reestablishment of sufficient insulation strength. The estimated fault distance and modelling of one-open-phase regime in symmetrical component coordinates is used as inputs for the detailed line model in phase coordinates, which in turn is used to determine the settings $S_{\mathrm{ABS}}$ and $S_{\mathrm{Re}2}$ (settings $S_{\mathrm{Re}}$ and $S_{\mathrm{Im}}$ are chosen above the noise level of the normal regime).

## 8.4. Testing of the Proposed Adaptive Automatic Reclosing Method

The proposed ASPAR method was tested on a 330 kV line model, which interconnects two 330 kV systems, S1 and S2, with short-circuit powers of 2 GVA and 1 GVA, and *X*/*R* ratios of 8 and 6. First, the performance of the proposed method was tested for various transient fault scenarios. The results including the time of arc extinction $t_{EXT}$, the full deionisation time according to (8.1) – $t_{\mathrm{DEION1}}$ –, the full deionisation time considering the maximum statistical necessary time from the moment of the arc extinction (60 ms) – $t_{\mathrm{DEION2}}$ –, the moment when the inner logic block AND4 with the 5 ms switch on delay is triggered (ASPAR operation will occur after 20 ms), $t_{\mathrm{AND4}}$, the moment when the final output command to reclose the CB is given, $t_{\mathrm{RECLOSE}}$, for positive and negative power flows are presented in Figs. 8.2 and 8.3 (zero time here corresponds to the beginning of the secondary arc). The constant setting recommendation is given for a comparison with the conventional AR shot method based on the empirical equation for deionisation time given in [140].

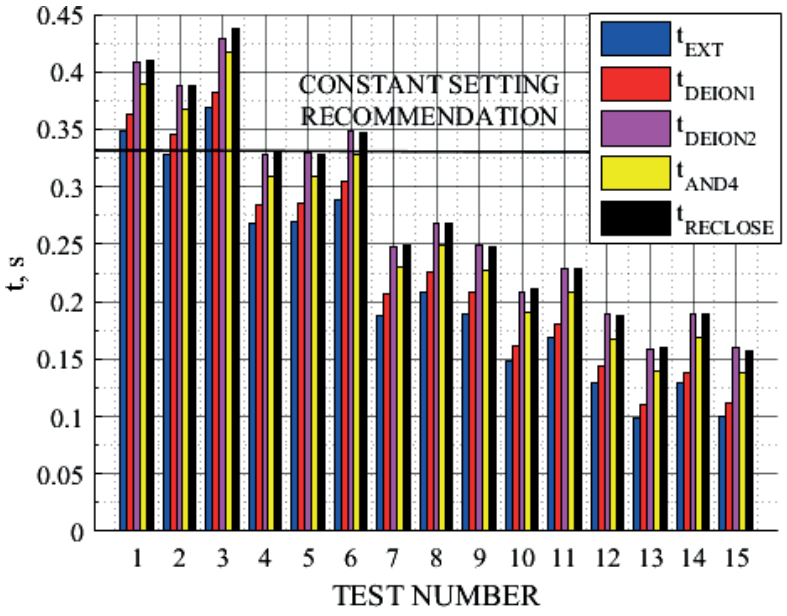


Fig. 8.2. The results of ASPAR testing for a positive pre-fault power flow [135].

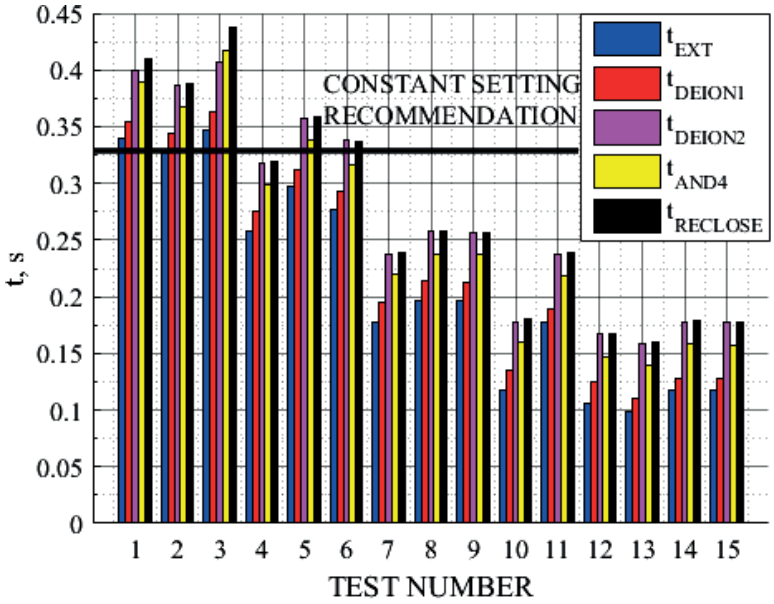


Fig. 8.3. The results of ASPAR testing for a negative pre-fault power flow [135].

The testing results show that in cases of delayed start of arc elongation process the constant SPAR setting may be insufficient, but the time difference will most probably be covered by additional time delays. However, for rapid arc elongation process scenarios there will be a significant unnecessary time gap between the moment of the actual deionisation and the reclosing command, which is not present for the proposed ASPAR method. These results also show that the reclose command of the proposed ASPAR method exceeds both analytical and statistical times of necessary deionisation times ($t_{DEION1}$, $t_{DEION2}$). Additionally, the proposed method successfully blocked SPAR operation in scenarios of permanent faults with high equivalent fault resistance in the amount of 5 kΩ.

## 8.5. Conclusions

1. The proposed model parameter estimation can be applied for other power system automation tasks such as creation of adaptive automation algorithms.
2. The proposed ASPAR algorithm applies topological analysis of a detailed three-phase steady-state line model during the dead time to calculate the adaptive setting, and the results of both parameter estimation stages from the proposed FL algorithm are used as inputs for this model.
3. The implemented dynamic primary and secondary fault arc models allowed to confirm the use of the real part of the faulted phase line-side voltage and discrete derivatives of the real and imaginary parts of the same voltage as suitable indications for fault arc extinction.
4. Testing of the described ASPAR algorithm showed the expected adaptive performance in cases of rapid fault arc elongation and blocking for permanent faults.

# CONCLUSIONS

1. The hypothesis of the Doctoral Thesis has been proven: the performance of the tested existing one-terminal-measurement-based FL and DP approaches was impaired when faults had a high transient resistance and they can be replaced by a technique based on a two-stage estimation of unknown power system model parameters that solves the problem as an optimisation task and expands the available measurements only within the controlled substation.
2. Measurements from both terminals of the line provide opportunities for fast and accurate FL, but their operation can be critically affected in case of loss of communication between substations or synchronisation of these measurements.
3. Most of the existing research on DP was more oriented towards various implementations of the DP itself in electromechanical, electronic or digital devices.
4. Most of the existing ASPAR methods ignore the influence of the healthy-phase power flow or they are highly dependent on accurate measurements of higher harmonic components or the DC offset, requiring a higher sampling frequency.
5. Fault regimes with multiple simultaneous asymmetries can be modelled by one complex equivalent circuit with electrical interconnections representing one of the asymmetries and iteratively recalculated EMF sources representing the other asymmetries or by interchanging calculation of regimes for two or more of such complex equivalent circuits where each circuit represents different asymmetry with electrical interconnections.
6. The presence of fault path resistance negatively affects the performance of the existing digital DP terminal both for L-L-E and L-E faults, especially in the case of fallen-tree faults, which can result in significant additional time delays.
7. The division of the model parameter estimation into two stages reduces the amount of unknown data that have to be determined after fault inception, thus making the second stage more feasible.
8. The accuracy of an existing digital FL using one-terminal measurements has a high degree of dependence on the pre-fault power flow, especially if it is oriented towards the substation, which is not present for the proposed applications of parameter estimation for DP and FL.
9. The initially tested modification of a randomised search provided satisfactory results, but it did require significant computation time, which led to the adoption of the GA.
10. One approach to the selection of measured parameters for use in the objective function is to sort them only by their sensitivity to changes in the fault distance, but it often results in objective functions with surface distortions and false extrema, which increases the risk of inaccurate fault distance estimation.
11. The updated version of the parameter estimation method using the GA clearly outperformed an existing one-terminal-measurement-based FL algorithm.

12. The updated version of the proposed method had higher maximum error values than the existing two-terminal-measurement-based FL method using NS quantities, but in terms of mean error and expected concentration of 95 % of fault distance estimation error values, the proposed method often outperformed the two-terminal-measurement-based method.
13. The proposed model parameter estimation can be applied for other power system automation tasks such as creation of adaptive automation algorithms.
14. Testing of the described ASPAR algorithm showed the expected adaptive performance in cases of rapid fault arc elongation and blocking for permanent faults.

# REFERENCES USED IN THE SUMMARY


1. A. Bratlov, I. Puusaar, M. Piironen, R. Stefansson, A. Maklakovs, V. Tarvydas and others (2019, Feb. 6). *ENTSOE Nordic and Baltic grid disturbance statistics 2017*. ENTSO-E Regional group Nordic. Available from:https://www.fingrid.fi/globalassets/dokumentit/fi/kantaverkko/suomen-sahkojarjestelma/hvac_2017_final_kotisivuille.pdf [Wieved: 6.09.2019 11:30].
2. V. Čuvičins un J. Priedīte. *Vadības sistēmas enerģētikā*. Rīga: RTU Izdevniecība, 2004, 229 lpp. ISBN:9984-32-441-9.
3. Я. Д. Баркан и Л. А. Орехов. *Автоматизация энергосистем: Учебное пособие для студентов вузов*. Москва: Высшая школа, 1981, 271 с.
4. А. Б. Барзам. *Систмная автоматика*. 4-е изд. Москва: Энергоатомиздат, 1989, 446 с. ISBN: 5-283-01024-4.
5. А. М. Федосеев и М. А. Федосеев. *Релейная защита электроэнергетических систем*. 2-е изд. Москва: Энергоатомиздат, 1992, 528 с. ISBN: 5-283-01171-2.
6. Н. И. Овчаренко. *Автоматика электрических станций и электроэнергетичеких систем: Учебник для вузов*. Москва: Издательство НЦ ЭНАС, 2000, 504 с. ISBN: 5-93196-020-1.
7. M. Bockarjova, A. Sauhats, and G. Andersson. Statistical algorithms for fault location on power transmission lines. In: *Proceedings 2005 IEEE Russia Power Tech conference,* St. Petersburg, Russia, 27–30 June 2005. Piscataway: IEEE, 2008, pp. 1–7, ISBN: 978-5-93208-034-4. Available from: DOI: 10.1109/PTC.2005.4524558.
8. M. Bockarjova, A. Dolgicers, and A. Sauhats. Enhancing fault location performance on power transmission lines. In: *Proceedings 2007 IEEE Lausanne Power Tech conference*, Lausanne, Switzerland, 1–5 July 2007. Piscataway: IEEE, 2008, pp. 1123–1128, ISBN: 978-1-4244-2189-3. Available from: DOI: 10.1109/PCT.2007.4538473.
9. A. Sauhats, A. Joņins un M. Bočkarjova. *Augstsprieguma līniju bojājuma vietas noteikšanas algoritmu sintēze*. Rīga: RTU EEF Enerģētikas institūts, 85 lpp. Pieejams: https://www.rtu.lv/writable/public_files/RTU_001.pdf.
10. J. Izykowski. *Fault location on power transmission lines*. Wroclaw: Printing House of Wroclaw University of Technology, 2008, p. 221. ISBN: 978-83-7493-430-5.
11. В. Л. Фабрикант. *Дистанционная защита*. Москва: Высшая школа, 1978, 215 с.
12. Э. М. Шнеерсон. *Цифровая релейная защита*. Москва: Энергоатомиздат, 2007, 549 с. ISBN: 978-5-283-03256-6.
13. G. Ziegler. *Numerical Distance Protection Principles and Applications*. 4th ed., Erlagen: Publicis, 2011, p.419. ISBN: 978-3-89578-381-4.
14. М. А. Беркович, В. А. Гладышев и В. А. Семенов. *Автоматика энергосистем*. Москва: Энергоатомиздат, 1991, 240 с. ISBN: 5-283-01004-X.
15. M. T. Sant and Y. G. Paithankar. Online digital fault locator for overhead transmission line. *Proceedings of the institution of Electrical Engineers*, vol. 126, No. 11, Nov. 1979, pp. 1181–1185. ISSN: 0020-3270. Available from: DOI: 10.1049/piee.1979.0201.
16. T. Takagi, Y. Yamakoshi, M. Yamaura, R. Kondow, and T. Matsushima. Development of a new type fault locator using the one-terminal voltage and current data. *IEEE Transactions on Power Apparatus and Systems*, vol. PAS-101, No. 8, Aug. 1982, pp. 2892–2898. ISSN: 0018-9510. Available from: DOI: 10.1109/TPAS.1982.317615.
17. L. C. Nicholson. Location of broken insulators and other transmission line troubles. *Transactions of the American Institute of Electrical Engineers*, vol. XXVI, No. 2, Jun. 1907, pp. 1319–1329. ISSN: 0096-3860. Available from: DOI: 10.1109/T-AIEE.1907.4764857.

18. AIEE Committee Report. Bibliography and summary of fault location methods. *Transactions of the American Institute of Electrical Engineers*. Part III: Power Apparatus and Systems, vol. 74, No. 3, Jan. 1955, pp. 1423–1428. ISSN: 0097-2460. Available from: DOI: 10.1109/AIEEPAS.1955.4499247.
19. T. W. Stringfield, D. J. Marihart, and R. F. Stevens. Fault location methods for Overhead lines. *Transactions of the American Institute of Electrical Engineers*. Part III: Power Apparatus and Systems, vol. 76, No. 4, Apr. 1957, pp. 518–529. ISSN: 0097-2460. Available from: DOI: 10.1109/AIEEPAS.1957.4499601.
20. F. J. Muench and G. A. Wright. Fault indicators: Types, strengths & applications. *IEEE Transactions on Power Apparatus and Systems*, vol. PAS-103, No. 12, Dec. 1984, pp. 3688–3693. ISSN: 0018-9510. Available from: DOI: 10.1109/TPAS.1984.318422.
21. K. Urasawa, K. Kanemaru, S. Toyota, and K. Sugiyama. New fault location system for power transmission lines using composite fiber-optic overhead ground wire (OPGW). *IEEE Transactions on Power Delivery*, vol. 4, No. 4, Oct. 1989, pp. 2005–2011. ISSN: 0885-8977. Available from: DOI: 10.1109/61.35624.
22. S. Jamali, A. Bahmanyar, and H. Borhani-Bahabadi. A fast and accurate fault location method for distribution networks with DG using genetic algorithms. In: *Proceedings 2015 Smart Grid Conference*, Teheran, Iran, 22–23 December 2015. Piscataway: IEEE, 2017, pp. 110–114, ISBN: 978-1-5090-0370-9. Available from: DOI: 10.1109/SGC.2015.7857419.
23. H. O. Cruz and F. B. Leão. Optimal placement of fault indicators using adaptive genetic algorithm. In: *Proceedings 2017 IEEE Power & Energy Society General Meeting*, Chicago, USA, 16–20 July 2017. Piscataway: IEEE, 2018, pp. 1–5, ISBN: 978-1-5386-2213-1. Available from: DOI: 10.1109/PESGM.2017.8273897.
24. Megger. *Fault finding solutions*, version MEG-231/mil/3m/11.2003, p. 44. Available from: http://www.unitronics-electric.com/pdf/articulos/FaultFindingBook_AG_en_V03.pdf [viewed 10.07.2019].
25. P. F. Gale, P. A. Crossley, X. Bingyin, G. Yaozhong, B. J. Cory, and J. R. G. Barker. Fault location based on travelling waves. In: *Proceedings 1993 Fifth International Conference on Developments in Power System Protection*, York, UK, 30 March to 2 April 1993. Piscataway: IEEE, 2002, pp. 54–59, ISBN: 0-85296-559-1.
26. F. F. Roberts. New methods for locating cable faults, particularly on high-frequency cables. *Journal of the Institution of Electrical Engineers- Part III: Radio and Communication Engineering*, vol. 93, No. 26, Nov. 1946, pp. 385–404. Available from: DOI: 10.1049/ji-3-2.1946.0067.
27. R. F. Stevens and T. W. Stringfield. Line-fault locator using fault-generated surges. *Electrical Engineering*, vol. 67, No. 11, Nov. 1948, pp. 1060–1060. ISSN: 0095-9197. Available from: DOI: 10.1109/EE.1948.6444437.
28. R. F. Stevens and T. W. Stringfield. A transmission line fault locator using fault-generated surges. *Transactions of the American Institute of Electrical Engineers*, vol. 67, No. 2, Jan. 1948, pp. 1168–1179. ISSN: 0096-3860. Available from: DOI: 10.1109/T-AIEE.1948.5059797.
29. M. Ando, E. O. Schweitzer, and R. A. Baker. Development and field-data evaluation of single-end fault locator for two-terminal HVDC transmission lines-Part 1: Data collection system and field data. *IEEE Transactions on Power Apparatus and Systems*, vol. PAS-104, No. 12, Dec. 1985, pp. 3524–3530. ISSN: 0018-9510. Available from: DOI: 10.1109/TPAS.1985.318905.

30. M. Ando, E. O. Schweitzer, and R. A. Baker. Development and field-data evaluation of single-end fault locator for two-terminal HVDC transmission lines-Part 2: algorithm and evaluation. *IEEE Transactions on Power Apparatus and Systems*, vol. PAS-104, No. 12, Dec. 1985, pp. 3531–3537. ISSN: 0018-9510. Available from: DOI: 10.1109/TPAS.1985.318906.
31. H. Lee and A. M. Mousa. GPS travelling wave fault locator systems: investigation into the anomalous measurements related to the lightning strikes. *IEEE Transactions on Power Delivery*, vol. 11, No. 3, Jul. 1996, pp. 1214–1223. ISSN: 0885-8977. Available from: DOI: 10.1109/61.517474.
32. M. M. Tawfik and M. M. Morcos. A fault locator for transmission lines based on Prony method. In: *Proceedings of 1999 IEEE Power Engineering Society Summer Meeting*, Edmonton, Canada, 18 July – 22 July, 1999. Piscataway: IEEE, 2002, pp. 943–947, ISBN: 0-7803-5569-5. Available from: 10.1109/PESS.1999.787443.
33. Q. Jian, C. Xiangxun, and Z. Jianchao. Travelling wave fault location of transmission line using wavelet transform. In *Proceedings of POWERCON 98. 1998 International Conference on Power System Technology*, Beijing, China, 18–21 August 1998. Piscataway: IEEE, 2002, pp. 533–537, ISBN: 0-7803-4754-4. Available from: DOI: 10.1109/ICPST.1998.729021.
34. O. Altay, E. Gursoy, A. Font, and O. Kalenderli. Travelling wave fault location on hybrid power lines. In: *Proceedings of 2016 IEEE International Conference on High Voltage Engineering and Application*, Chengdu, China, 19–22 September 2016. Piscataway: IEEE, 2016, pp. 1–4, ISBN: 978-1-5090-0497-3. Available from: DOI: 10.1109/ICHVE.2016.7800719.
35. A. M. Abeid, H. A. Abd el-Ghany, A. M. Azmy. An advanced travelling-wave fault-location algorithm for simultaneous faults. In: *Proceedings of 2017 Nineteenth International Middle East Power Systems Conference*, Cairo, Egypt, 19–21 December 2017. Piscataway: IEEE, 2018, pp. 747–752, ISBN: 978-1-5386-0991-0. Available from: DOI: 10.1109/MEPCON.2017.8301265.
36. H. P. Dupuis and W. E. Jacobs. Fault location and relay performance analysis by automatic oscillographs. *Transactions of the American Institute of Electrical Engineers*, vol. 65, No. 7, Jul. 1946, pp. 442–446. ISSN: 0096-3860. Available from: DOI: 10.1109/T-AIEE.1946.5059367.
37. A. C. Lee, Ground-fault-location indicator. *Transactions of the American Institute of Electrical Engineers. Part* III: *Power Apparatus and Systems*, vol. 76, No. 3, Apr. 1957, pp. 1370–1372. ISSN: 0097-2460. Available from: DOI: 10.1109/AIEEPAS.1957.4499796.
38. S. E. Westlin and J. A. Bubenko. An accurate method for fault location on electric power transmission lines. *IFAC Proceedings Volumes*, Melnbourne, Australia, 21–25 February 1977, vol. 10, No. 1, Feb. 1977, pp. 262–266. Available from: DOI: 10.1016/S1474-6670(17)67067-8.
39. L. Eriksson, M. M. Saha, and G. D. Rockefeller. An accurate fault locator with compensation for apparent reactance in the fault resistance resulting from remote-end infeed. *IEEE Transactions on Power Apparatus and Systems*, vol. PAS-104, No. 2, Feb. 1985, pp. 424–436. ISSN: 0018-9510. Available from: DOI: 10.1109/TPAS.1985.319058.
40. A. T. Johns, S. Jamali, and S. M. Haden. New accurate transmission line fault location equipment. In: *Proceedings of 1989 Fourth International Conference on Developments in Power Protection*, Edinburgh, UK, 11–13 April 1989. Piscataway: IEEE, 2002, pp. 1–5.
41. J. A. Jiang, Y. H. Lin, C. W. Liu, J. Z. Yang, and T. M. Too. An adaptive fault locator system for transmission lines. In: *Proceedings of 1999 IEEE Power Engineering Society Summer Meeting*, Edmonton, Canada, 18–22 July 1999. Piscataway: IEEE, 2002, pp. 930–936, ISBN: 0-7803-5569-5. Available from: DOI: 10.1109/PESS.1999.787441.

42 J. A. Jiang, J. Z. Yang, Y. H. Lin, C. W. Liu, and J. C. Ma. An adaptive PMU based fault detection/location technique for transmission lines. I. Theory and Algorithms, *IEEE Transactions on Power Delivery*, vol. 15, No. 2, Apr. 2000, pp. 486–493.ISSN: 0885-8977. Available from: DOI: 10.1109/61.852973.

43. J. A. Jiang, Y. H. Lin, J. Z. Yang, T. M. Too, and C. W. Liu. An adaptive PMU based fault detection/location technique for transmission lines. II. PMU implementation and performance evaluation. *IEEE Transactions on Power Delivery*, vol. 15, No. 4, Oct. 2000, pp. 1136–1146. ISSN: 0885-8977. Available from: DOI: 10.1109/61.891494.
44. M. Joorabian. Artificial neural network based fault locator for EHV transmission system. In: *Proceedings of 2000 10th Mediterranean Electrotechnical Conference*, Lemesos, Cyprus, 29–31 May 2000. Piscataway: IEEE, 2002, pp. 1003–1006, ISBN: 0-7803-6290-X. Available from: DOI: 10.1109/MELCON.2000.879703.
45. M. Kezunovic and M. Knezev. Selection of optimal fault location algorithm. In: *Proceedings 2008 IEEE Power and Energy Society General Meeting – Conversion and Delivery of Electrical Energy in the 21st Century*, Pittsburg, USA, 20–24 July 2008. Piscataway: IEEE, 2008, pp. 1–5, ISBN: 978-1-4244-1905-0. Available from: DOI: 10.1109/PES.2008.4596775.
46. A. S. Altaie and J. Asumandu. Fault location using a new control technique, multiple classifier, and artificial neural network. In: *Proceedings 2017 IEEE Texas Power and Energy conf*erence, College Station, USA, 9–10 February 2017. Piscataway: IEEE, 2017, pp. 1–6, ISBN: 978-1-5090-6618-6. Available from: DOI: 10.1109/TPEC.2017.7868267.
47. C. E. M. Pereira and L. C. Zanetta. Optimization algorithm for fault location in transmission lines considering current transformer saturation. *IEEE Transactions Power Delivery*, vol. 20, No. 2, Apr. 2005, pp. 603–608. ISSN: 0885-8977. Available from: DOI: 10.1109/TPWRD.2004. 838521.
48. Z. Jian, Z. HongJun, and Q. JiangFeng. A two-terminal fault location algorithm using asynchronous sampling based on genetic algorithm. In: *Proceedings 2011 International Conference on Advanced Power System Automation and Protection*, Beijing, China, 16–20 October 2011. Piscataway: IEEE, 2012, vol. 2, pp. 1513–1516, ISBN: 978-1-4244-9622-8. Available from: DOI: 10.1109/APAP.2011.6180605.
49. M. G. Davoudi, J. Sadeh, and K. Kamyab. Time domain fault location on transmission lines using genetic algorithm. In: *Proceedings 2012 11th International Conference on Environment and Electrical Engineering*, Venice, Italy, 18–25 May 2012. Piscataway: IEEE, 2012, pp. 1087–1092, ISBN: 978-1-4577-1830-4. Available from: DOI: 10.1109/EEEIC.2012.6221542.
50. A. S. Ahmed, M. A. Attia, N. M. Hamed, and A. Y. Abdelaziz. Comparison between genetic algorithm and whale optimization algorithm in fault location estimation in power systems. In: *Proceedings 2017 Nineteenth International Middle East Power Systems Conference*, Cairo, Egypt, 19–21 December 2017. Piscataway: IEEE, 2018, pp. 631–637, ISBN: 978-1-5386-0991-0. Available from: DOI: 10.1109/MEPCON.2017.8301247.
51. А. М. Федосеев. *Релейная защита электрических систем*. Москва: Государственное энергетическое издательство, 1952, 480 с.
52. W. A. Elmore. *Protective relaying theory and applications*. 2nd edition, New York: Marcel Dekker, 2003, p. 432. ISBN: 978-0824709723.
53. L. Hewitson, M. Brown, R. Balakrishnan. *Practical Power System Protection*. Oxford: Newnes, 2004, p. 288. ISBN: 0 7506 6397 9.
54. J. L. Blackburn and J. T. Domin. *Protective Relaying*. 3rd edition, New York: CRC Press, 2006, p. 664. ISBN: 978-1-57444-716-3.

55. L. N. Crichton. The distance relay for automatically sectionalizing electrical net works. *Transactions of the American Institute of Electrical Engineers*, vol. XLII, pp. 527–537, Jan. 1923. ISSN: 0096-3860. Available from: DOI: 10.1109/T-AIEE.1923.5060893.
56. H. A. McLaughlin and E. O. Erickson. The impedance relay developments and application. *Transactions of the American Institute of Electrical Engineers*, vol. 47, No.3, Jul. 1928, pp. 776–782. ISSN: 0096-3860. Available from: DOI: 10.1109/T-AIEE.1928.5055053.
57. L. N. Crichton. High-speed protective relays. *Transactions of the American Institute of Electrical Engineers*, vol. 49, No. 4, Oct. 1930, pp. 1232–1239. ISSN: 0096-3860. Available from: DOI: 10.1109/T-AIEE.1930.5055649.
58. W. A. Lewis and L. S. Tippet. Fundamental basis for distance relaying. *Electrical Engineering*, vol. 50, No. 6, Jun. 1931, pp. 420–422. ISSN: 0095-9197. Available from: DOI: 10.1109/EE.1931.6430279.
59. S. L. Goldsborough and R. M. Smith. A new distance ground relay. *Transactions of the American Institute of Electrical Engineers*, vol. 55, No. 6, Jun. 1936, pp. 697–703. ISSN: 0096-3860. Available from: DOI: 10.1109/T-AIEE.1936.5057333.
60. L. J. Audlin and A. R. Van C. Warrington. Distance relay protection for subtransmission line made economical. *Electrical Engineering*, vol. 62, No. 9, Sept. 1943, pp. 574–578. ISSN: 0095-9197. Available from: DOI: 10.1109/EE.1943.6435918.
61. M. A. Bostwick and E. L. Harder. Relay protection of tapped transmission lines. *Transactions of the American Institute of Electrical Engineers*, vol. 62, No. 10, Oct. 1943, pp. 645–650. ISSN: 0096-3860. Available from: DOI: 10.1109/T-AIEE.1943.5058619.
62. S. L. Goldsborough. A distance relay with adjustable phase-angle discrimination. *Transactions of the American Institute of Electrical Engineers*, vol. 63, No. 11, Nov. 1944, pp. 835–838. ISSN: 0096-3860. Available from: DOI: 10.1109/T-AIEE.1944.5058808.
63. E. Clarke. Impedances seen by relays during power swings with and without faults. *Transactions of the American Institute of Electrical Engineers*, vol. 64, No. 6, Jun. 1945, pp. 372–384. ISSN: 0096-3860. Available from: DOI: 10.1109/T-AIEE.1945.5059154.
64. A. R. Van C. Warrington. Graphical method for estimating the performance of distance relays during faults and power swings. *Transactions of the American Institute of Electrical Engineers*, vol. 68, No. 1, Jul. 1949, pp. 608–621. ISSN: 0096-3860. Available from: DOI: 10.1109/T-AIEE.1949.5059984.
65. F. R. Bergseth. An electronic distance relay using a phase-discrimination principle. *Transactions of the American Institute of Electrical Engineers*, vol. 73, No. 2, Jan. 1954, pp. 1276–1279. ISSN: 0097-2460. Available from: DOI: 10.1109/AIEEPAS.1954.4498958.
66. C. Adamson and L. M. Wedepohl. Power system protection, with particular reference to the application on junction transistors to distance relays. *Proceedings of the IEE – Part A: Power Engineering*, vol. 103, No. 10, Aug. 1956, pp. 379–388. ISSN: 0369-8882. Available from: DOI: 10.1049/pi-a.1956.0106.
67. W. K. Sonnemann and H. W. Lensner. Compensator distance relaying 1. General principles of Operation. *Transactions of the American Institute of Electrical Engineers. Part III: Power Apparatus and Systems*, vol. 77, No. 3, Apr. 1958, pp. 372–382. ISSN: 0097-2460. Available from: DOI: 10.1109/AIEEPAS.1958.4499939.
68. W. E. Rich and H. J. Calhoun. Compensator distance relaying 2. Design and performance. *Transactions of the American Institute of Electrical Engineers. Part III: Power Apparatus and Systems*, vol. 77, No. 3, Apr. 1958, pp. 383–387. ISSN: 0097-2460. Available from: DOI: 10.1109/AIEEPAS.1958.4499940.

69. K. Parthasarathy. Three-system and single-system static distance relays. *Proceedings of the Institution of Electrical Engineers*, vol. 113, No. 4, Apr. 1966, pp. 641–651. ISSN: 0020-3270. Available from: DOI: 10.1049/piee.1966.0104.
70. N. M. Anil Kumar. New approach to distance relays with quadrilateral polar characteristic for e.h.v.-line protection. *Proceedings of the Institution of Electrical Engineers*, vol. 117, No. 10, Oct. 1970, pp. 1986–1992. ISSN: 0020-3270. Available from: DOI: 10.1049/piee.1970.0350.
71. V. T. Ingole, M. T. Sant, and Y. G. Paithankar. New technique for quadrilateral distance relay. *Proceedings of the Institution of Electrical Engineers*, vol. 121, No. 6, Jun. 1974, pp. 464–466. ISSN: 0020-3270. Available from: DOI: 10.1049/piee.1974.0112.
72. B. J. Mann and I. F. Morrison. Digital calculation of impedance for transmission line protection. *IEEE Transactions on Power Apparatus and Systems*, vol. PAS-90, No. 1, Jan. 1971, pp. 270–279. ISSN: 0018-9510. Available from: DOI: 10.1109/TPAS.1971.292966.
73. G. B. Gilcrest, G. D. Rockefeller, and E. A. Udren. High-speed distance relaying using a digital computer I – System description. *IEEE Transactions on Power Apparatus and Systems*, vol. PAS-91, No. 3, May 1972, pp. 1235–1243. ISSN: 0018-9510. Available from: DOI: 10.1109/TPAS.1972.293482.
74. G. D. Rockefeller and E. A. Udren. High-speed distance relaying using a digital computer II – Test results. *IEEE Transactions on Power Apparatus and Systems*, vol. PAS-91, No. 3, May 1972, pp. 1244–1258. ISSN: 0018-9510. Available from: DOI: 10.1109/TPAS.1972.293483.
75. P. G. McLaren and M. A. Redfern. Fourier-series techniques applied to distance protection. *Proceedings of the Institution of Electrical Engineers*, vol. 122, No. 11, Nov. 1975, pp. 1301–1305. ISSN: 0020-3270. Available from: DOI: 10.1049/piee.1975.0316.
76. A. G. Phadke, T. Hlibka, M. Ibrahim, and M. G. Adamiak. A microcomputer based symmetrical component distance relay. In: *IEEE Conference Proceedings Power Industry Computer Applications Conference*, Cleveland, USA, 15–19 May, 1979. Piscataway: IEEE, 2002, pp. 47–55. Available from: DOI: 10.1109/PICA.1979.720045.
77. S. P. Patra, S. K. Basu, and S. Choudhuri. Analysis of phase-sequence detector for polyphase distance relay. *Proceedings of the Institution of Electrical Engineers*, vol. 119, No. 10, Oct. 1972, pp. 1503–1504. ISSN: 0020-3270. Available from: DOI: 10.1049/piee.1972.0297.
78. U. S. Hazra, S. K. Basu, and S. Chowdhuri. Polyphase distance relay by 6-input phase-sequence detector. *Proceedings of the Institution of Electrical Engineers*, vol. 123, No. 10, Oct. 1976, pp. 1017–1020. ISSN: 0020-3270. Available from: DOI: 10.1049/piee.1976.0226.
79. A. T. Johns and A. A. El-Alaily. New distance protective relay with improved coverage for high-resistance earth faults. *Proceedings of the Institution of Electrical Engineers*, vol. 124, No. 4, Apr. 1977, pp. 349–355. ISSN: 0020-3270. DOI: 10.1049/piee.1977.0064.
80. P. A. Crossley and P. G. McLaren. Distance protection based on travelling waves. *IEEE Transactions on Power Apparatus and Systems*, vol. PAS-102, No. 9, Sept. 1983, pp. 2971–2983. ISSN: 0018-9510. Available from: DOI: 10.1109/TPAS.1983.318102.
81. Y. Ohura, T. Matsuda, M. Suzuki, F. Andow, Y. Kurosawa, and A. Takeuchi. A digital distance relay using negative sequence current. *IEEE Transactions on Power Delivery*, vol. 5, No. 1, Jan. 1990, pp. 79–84. ISSN: 0885-8977. Available from: DOI: 10.1109/61.107259.
82. Z. Zhizhe and C. Deshu. An adaptive approach in digital distance protection. *IEEE Transactions on Power Delivery*, vol. 6, No. 1, Jan. 1991, pp. 135–142. ISSN: 0885-8977. Available from: DOI: 10.1109/61.103732.

83. Y. Q. Xia, K. K. Li, and A. K. David. Adaptive relay setting for stand-alone digital protection, *IEEE Transactions on Power Delivery*, vol. 9, No. 1, Jan. 1994, pp. 480–491. ISSN: 0885-8977. Available from: DOI: 10.1109/61.277720.
84. P. G. McLaren, G. W. Swift, Z. Zhang, E. Dirks, R. P. Jayasinghe, and I. Fernando. A new positive sequence directional element for numerical distance relays. In: *Proceedings IEEE WESCANEX 95. Communications, Power and Computing conference*, Winnipeg, Canada, 15–16 May 1995. Piscataway: IEEE, 2002, pp. 334–339, ISBN: 0-7803-2725-X. Available from: DOI: 10.1109/WESCAN.1995.494051.
85. A. Apostolov. Implementation of a transient energy method for directional detection in numerical distance relays. In: *Proceedings 1999 IEEE Transmission and Distribution Conference*, New Orleans, USA, 11–16 April 1999. Piscataway: IEEE, 2002, pp. 382–387, ISBN: 0-7803-5515-6. Available from: DOI: 10.1109/TDC.1999.755382.
86. S. H. Kang, K. H. Kim, K. R. Cho, and J. K. Park. High speed offset free distance relaying algorithm using multilayer feedforward neural networks. In: *Proceedings of International Conference on Intelligent System Application to Power Systems*, Orlando, USA, 28 January to 2 February 1996. Piscataway: IEEE, 2002, pp. 210–214, ISBN: 0-7803-3115-X. Available from: DOI: 10.1109/ISAP.1996.501070.
87. S. J. Lee and C. C. Liu. Intelligent approach to coordination identification in distance relaying. In: *Proceedings of International Conference on Intelligent System Application to Power Systems*, Orlando, USA, 28 January to 2 February 1996. Piscataway: IEEE, 2002, pp. 62–67, ISBN: 0-7803-3115-X. Available from: DOI: 10.1109/ISAP.1996.501045.
88. J. P. de Sa, J. Afonso, and R. Rodrigues. A Probabilistic approach to setting distance relays in transmission networks. *IEEE Transactions on Power Delivery*, vol. 12, No. 2, Apr. 1997, pp. 681–686. ISSN: 0885-8977. Available from: DOI: 10.1109/61.584342.
89. A. S. AlFuhaid and M. A. El-Sayed. A recursive least-squares digital distance relaying algorithm. *IEEE Transactions on Power Delivery*, vol. 14, No. 4, Oct. 1999, pp. 1257–1262. ISSN: 0885-8977. Available from: DOI: 10.1109/61.796215.
90. K. K. Li, L. L. Lai, and A. K. David. Stand alone intelligent digital distance relay. *IEEE Transactions on Power Systems*, vol. 15, No. 1, Feb. 2000, pp. 137–142. ISSN: 0885-8950. Available from: DOI: 10.1109/59.852112.
91. S. Jamali. A fast adaptive digital distance protection. In: *Proceedings 2001 Seventh International Conference on Developments in Power System Protection (IEE)*, Amsterdam, Netherlands, 9–12 April 2001. Piscataway: IEEE, 2002, pp. 149–152, ISBN: 0-85296-732-2. Available from: DOI: 10.1049/cp:20010122.
92. T. Segui, P. Bertrand, M. Guillot, P. Hanchin, and P. Bastard. Fundamental basis for distance relaying with parametrical estimation. *IEEE Transactions on Power Delivery*, vol. 15, No. 2, Apr. 2000, pp. 659–664. ISSN: 0885-8977. Available from: DOI: 10.1109/61.853001.
93. C. S. Chen, C. W. Liu, and J. A. Jiang. Application of combined adaptive Fourier filtering technique and fault detector to fast distance protection. *IEEE Transactions on Power Delivery*, vol. 21, No. 2, Apr. 2006, pp. 619–626. ISSN: 0885-8977. Available from: DOI: 10.1109/TPWRD.2005.858808.
94. M. Bockarjova, A. Sauhats, and G. Andersson. Statistical algorithm for power transmission lines distance protection. In: *Proceedings 2006 Probabilistic Methods Applied to Power Systems conf*erence, Stockholm, Sweden, 11–15 June 2006. Piscataway: IEEE, 2007, pp. 1–7, ISBN: 978-91-7178-585-5. Available from: DOI: 10.1109/PMAPS.2006.360210.

95. E. Sorrentino and V. De Andrade. Optimal-probabilistic method to compute the reach settings of distance relays. *IEEE Transactions on Power Delivery*, vol. 26, No. 3, Jul. 2011, pp. 1522–1529. ISSN: 0885-8977. Available from: DOI: 10.1109/TPWRD.2010.2091724.
96. K. Jia, T. Bi, W. Li, and Q. Yang. Ground fault distance protection for paralleled transmission lines. *IEEE Transactions on Industry Applications*, vol. 51, No. 6, Nov.–Dec. 2015, pp. 5228–5236. ISSN: 0093-9994. Available from: DOI: 10.1109/TIA.2015.2416243.
97. W. Chen, Z. Hao, J. Guan, Y. Dang, D. Du, and X. Wang. Research on the distance protection performance for untransposed parallel transmission lines based on six-phase parameter information. In: *Proceedings 2016 IEEE 16th International Conference on Environmental and Electrical Engineering*, Florence, Italy, 7–10 June 2016. Piscataway: IEEE, 2016, pp. 1–6, ISBN: 978-1-5090-2321-9. Available from: DOI: 10.1109/EEEIC.2016.7555406.
98. C. Lozaro, J. P. Marquez, G. Marchesan, and G. C. Junior. Waveform asymmetry of instantaneous current signal based symmetrical fault detection during power swing. *Electric Power Systems Research*, vol. 155, Feb. 2018, pp. 340–349. ISSN: 0378-7796. Available from: https://doi.org/10.1016/j.epsr.2017.11.005.
99. S. M. Hashemi and M. S. Pasand. Distance protection during asymmetrical power swings: Challenges and solutions. *IEEE Transactions on Power Delivery*, vol. 33, No. 6, Dec. 2018, pp. 2736–2745. ISSN: 0885-8977. Available from: DOI: 10.1109/TPWRD.2018.2816304.
100. S. Biswas and P. K. Nayak. An unblocking assistance to distance relays protecting TCSC compensated transmission lines during power swing. *International Transactions on Electrical Energy Systems*, vol. 29, No. 8, Apr. 2019, pp. 1–21. ISSN: 2050-7038. Available from: https://doi.org/10.1002/2050-7038.12034.
101. Н. Н. Беляков, К. П. Кадомская, М. Л. Левинштейн и др. *Процессы при однофазном автоматическом повторном включении линий высоких напряжений*. Москва: Энергоатомиздат, 1991, 256 с. ISBN: 5-283-01184-4.
102. M. Djuric, Z. Radojevic, and K. Zoric. Determination of the arc extinction time on power lines using voltage signals. *ETEP*, vol. 12, No. 6, Nov./Dec. 2002, pp. 415–418. ISSN: 2050-7038. Available from: https://doi.org/10.1002/etep.4450120605.
103. D. S. Fitton, R. W. Dunn, R. K. Aggarwal, A. T. Johns, and A. Bennett. Design and implementation of an adaptive single pole autoreclosure technique for transmission lines using artificial neural networks. *IEEE Transactions on Power Delivery*, vol. 11, No. 2, Apr. 1996, pp. 748–756. ISSN: 0885-8977. Available from: DOI: 10.1109/61.489331.
104. S. P. Ahn, C. H. Kim, R. K. Aggarwal, and A. T. Johns. An alternative approach to adaptive single pole auto-reclosing in high voltage transmission systems based on variable dead time control. *IEEE Transactions on Power Delivery*, vol. 16, No. 4, Oct. 2001, pp. 676–686. ISSN: 0885-8977. Available from: DOI: 10.1109/61.956756.
105. P. Upadhyay, L. Heistrene, and S. Chandrasekaran. Design and implementation of adaptive autoreclosure for EHV transmission line. In: *Proceedings 2016 International Conference on Microelectronics, Computing and Communications (MircoCom)*, Durgapur, India, 23–25 January 2016. Piscataway: IEEE, 2016, pp. 1–6, ISBN: 978-1-4673-6622-9. Available from: DOI: 10.1109/MicroCom.2016.7522588.
106. B. Mahamedi. An adaptive single-pole auto-reclosing function. In: *Proceedings 2012 06th Power Systems Protection & Control Conference (PSPC06)*, Teheran, Iran, 3 January 2012. Teheran: Iranian Association of Electrical &Electronics Engineers, 2012, pp. 1–5. Available from: http://www.ipaps.ir/files/archive/6/Arc6_259.pdf [viewed 10.09.2019].

107. K. M. C. Dantas, W. L. A. Neves, and D. Fernandes. An Approach for controlled reclosing of shunt-compensated transmission lines. *IEEE Transactions on Power Delivery*, vol. 29, No. 3, Jun. 2014, pp. 1203–1211. ISSN: 1932-5517. Available from: DOI: 10.1109/TPWRD.2013.2289394.
108. X. Luo, C. Huang, Y. Jiang, and S. Guo. An adaptive three-phase reclosure scheme for shunt reactor-compensated transmission lines based on the change of current spectrum. *Elsevier Electric Power Systems Research*, vol. 158, May 2018, pp. 184–194. ISSN: 0378-7796. Available from: https://doi.org/10.1016/j.epsr.2018.01.011.
109. A. Dolgicers and I. Zalitis. Numerical calculation method for symmetrical component analysis of multiple simultaneous asymmetrical faults. In: *Proceedings 2017 IEEE 58th International Scientific Conference on Power and Electrical Engineering of Riga Technical University*, Riga, Latvia, 12–13 October 2017. Piscataway: IEEE, 2017, pp. 1–7, ISBN: 978-1-5386-3847-7. Available from: DOI: 10.1109/RTUCON.2017.8124748.
110. G. I. Atabekov. *The Relay protection of High Voltage Networks*, London: Pergamon Press, 1960, p. 576.
111. С. А. Ульянов. Электромагнитные переходные процессы в электрических системах. Москва: Энергия, 1970, 520 с.
112. E. Clarke. *Circuit analysis of A-C power systems*, New York: Wiley, 1943, p. 936.
113. Л. А. Бессонов. *Теоретические основы электротехники. Электрические цепи: Учебник для электротехнических, энергетических, приборостроительных специальностей вузов*. 9-е изд. Москва: Высшая школа, 1996, 638 с. ISBN: 5-06-002160-2.
114. A. Agarwal and J. H. Lang. *Foundations of analog and electronic circuits*, San Francisco: Morgan Kaufmann Publishers, 2005, p. 1008. ISBN: 1-55860-735-8.
115. A. Dolgicers and J. Kozadajevs. Phase plane usage for convergence analysis of Seidel method applied for network analysis. In: *Proceedings 2014 IEEE 2nd Workshop on Advances in Information, Electronic and Electrical Engineering*, Vilnius, Lithuania, 28–29 November, 2014. Piscataway: IEEE, 2015, pp. 1-6, ISBN: 978-1-4799-7122-0. Available from: DOI: 10.1109/AIEEE.2014.7020321.
116. А. А. Самарский, А. В. Гулин. *Введение в численные методы*. Москва: Наука, 1987, 286 с.
117. S. C. Chapra and R. P. Canale. *Numerical methods for engineers*. 6th ed., London: McGraw-Hill Higher Education, 2010, p. 960.
118. В. И. Крылов, Н. С. Скобля. *Методы приближенного преобразования Фурье и обращения преобразования Лапласа. Справочная книга*. Москва: Наука, 1974, 224 с.
119. Б. А. Калабеков, В. Ю. Лапидус, В. М. Малафеев. *Методы автоматизированного расчета электронных схем в технике связи*. Москва: Радио и связь, 1990, 272 с. ISBN:5-256-00674-6.
120. P. Taklaja, R. Oidram, J. Niitsoo, and I. Palu. Causes of indefinite faults in Estonian 110 kV overhead power grid. *Oil Shale*, vol. 30, No. 2S, 2013, pp. 225-243. ISSN: 0208-189X. Available from: DOI: 10.3176/oil.2013.2S.04.
121. S. Šeikins. Pārejas pretestības ietekme uz distances aizsardzību. Maģistra darbs, Rīga: RTU, 2014, 72. lpp.
122. M. Silarajs, A. Utans, L. Leite, and A. Sauhats. Multifunction relay protection device for power transmission lines LIDA. In: *Proceedings 2007 The 2nd International conference on Electrical and Control Technologies*, Kaunas, Lithuania, 3–4 May 2007. Kaunas: Kaunas University Of Technology, 2007, pp. 120–125, ISBN: 978-1-6343-9796-4. Available from: http://www.proceedings.com/25048.html [viewed 10.09.2019].

123. I. Zalitis, A. Dolgicers, and J. Kozadajevs. Experimental testing of distance protection performance in transient fault path resistance environment. In: *Proceedings 2017 5th IEEE Workshop on Advances in Information, Electronic and Electrical Engineering*, Riga, Latvia, 24–25 November 2017. Piscataway: IEEE, 2018, pp. 1–6, ISBN: 978-1-5386-4138-5. Available from: DOI: 10.1109/AIEEE.2017.8270526.
124. W. C. New. Combined phase and ground distance relaying. *Transactions of the American Institute of Electrical Engineers*, vol. 69, No. 1, Jan. 1950, pp. 37–44. ISSN: 0096-3860. Available from: DOI: 10.1109/T-AIEE.1950.5060117.
125. I. Zalitis, A. Dolgicers, J. Kozadajevs. A distance protection based on the estimation of system model parameters. In: *Proceedings 2017 IEEE Manchester PowerTech*, Manchester, UK, 18–22 June 2017. Piscataway: IEEE, 2017, pp. 1–6, ISBN: 978-1-5090-4238-8. Available from: DOI: 10.1109/PTC.2017.7981277.
126. I. Zalitis, A. Dolgicers, J. Kozadajevs. A power transmission line fault locator based on the estimation of system model parameters. In: *Proceedings 2017 IEEE International Conference on Environment and Electrical Engineering*, Milan, Italy, 6–9 June 2017. Piscataway: IEEE, 2017, pp. 1–6, ISBN: 978-1-5386-3918-4. Available from: DOI: 10.1109/EEEIC.2017.7977459.
127. S. S. Geramian, H. A. Abyane, and K. Mazlumi. Determination of optimal PMU placement for fault location using genetic algorithm. In: *Proceedings 2008 13th International Conference on Harmonics and Quality of Power*, Wollongong, Australia, 28 September to 1 October 2008. Piscataway: IEEE, 2008, pp. 1–5, ISBN: 978-1-4244-1771-1. Available from: DOI: 10.1109/ICHQP.2008.4668810.
128. L. He, K. Jia, and Z. Fan. The immune genetic algorithm in fault diagnosis of modern power system. In: *Proceedings 2010 2nd International Conference on Education Technology and Computer*, Shanghai, China, 22–24 June 2010. Piscataway: IEEE, 2010, pp. 26–29, ISBN: 978-1-4244-6367-1. Available from: DOI: 10.1109/ICETC.2010.5529742.
129. Л. А. Гладков, В. В. Курейчик, В. М. Курейчик. *Генетические алгоритмы*. *Учебное пособие*. 2-е изд. Москва: Физматлит, 2006, 320 с. ISBN: 5-9221-0510-8.
130. Т. В. Панченко. *Генетические алгоритмы*. *Учебно-методическое пособие*. Астрахань: АГУ, 2007, 87 с. ISBN: 5-88200-913-8.
131. I. Plummer. *Asymmetry in distribution systems: causes, harmful effects and remedies*. M. Sc. Eng. thesis, Dept. Electrical and Computer Engineering, Louisiana State University and Agricultural and Mechanical College, Louisiana, 2011, p. 130. Available from: https://digitalcommons.lsu.edu/cgi/viewcontent.cgi?article=2489&context=gradschool_theses [viewed 12.09.2019].
132. *Нормы качества электрической энергии в системах электроснабжения общего назначения*, ГОСТ 32144-2013, Март 2013, 20 с. Доступно: https://www.elec.ru/files/2014/05/06/GOST-32144-2013-Elektricheskaja-energija.pdf.
133. C. Preve. *Protection of electrical networks*, London: ISTE Ltd., 2006, p. 508. ISBN: 978-1-905209-06-4.
134. D. P. Kothari and I. J. Nagrath. *Modern Power System Analysis*, New Delhi: Tata McGraw Hill Education Private Limited, 3rd. ed., 2009, p. 694. ISBN: 978-0-07-049489-3.
135. I. Zalitis, A. Dolgicers, J. Kozadajevs. An adaptive single-pole automatic reclosing method for uncompensated high-voltage transmission lines. *Electric Power Systems Research*, vol. 166, Jan. 2019, pp. 210–222. ISSN: 0378-7796. Available from: https://doi.org/10.1016/j.epsr.2018.10.012.

136. C. F. Wagner, R. D. Evans. *Symmetrical components as applied to the analysis of unbalanced electrical circuits*. 1st ed., New York: McGraw-Hill, p. 437, 1933.
137. E. R. Bussy, N. M. Ljumb, and A. C. Britten. Effect of ADLash optical fibre cable on corona inception gradient and electric fields around the earth wire of the Apollo-Cahora Bassa HVDC transmission line. In: *Proceedings 2004 IEEE AFRICON. 7th Africon Conference*, Gaborone, Botswana, 15–17 September 2004. Piscataway: IEEE, 2005, pp. 607–612, ISBN: 0-7803-8605-1. Available from: DOI: 10.1109/AFRICON.2004.1406751.
138. A. T. Johns and A. M. Al-Rawi. Digital simulation of EHV systems under secondary arcing conditions associated with single-pole autoreclosure. *IEE Proceedings C-Generation, Transmission and Distribution*, vol. 129, No. 2, Mar. 1982. pp. 49–58. ISSN: 0143-7046. Available from: DOI: 10.1049/ip-c.1982.0009.
139. A. T. Johns, R. K. Aggarwal, and Y. H. Song. Improved techniques for modelling fault arcs on faulted EHV transmission systems. *IEE Proceedings C-Generation, Transmission and Distribution*, vol. 141, No. 2, Mar. 1994, pp. 148–154. ISSN: 1350-2360. Available from: DOI: 10.1049/ip-gtd:19949869.
140. A. Pereira, F. Perez-Yauli, F. L. Quilumba. Three-phase recloser time delays determination in 138 kV and 46 kV lines of the Empresa Electrica Quito. In: *Proceedings 2017 IEE Second Ecuador Technical Chapters Meeting (ETCM)*, Gaborone, Botswana, 16–20 October 2017. Piscataway: IEEE, 2018, pp. 1–6, ISBN: 978-1-5386-3895-8. Available from: DOI: 10.1109/ETCM.2017.8247514.